

University of Groningen

[18F]FDG-PET/CT Radiomics and Artificial Intelligence in Lung Cancer

Manafi-Farid, Reyhaneh; Askari, Emran; Shiri, Isaac; Pirich, Christian; Asadi, Mahboobeh; Khateri, Maziar; Zaidi, Habib; Beheshti, Mohsen

Published in:
 Seminars in Nuclear Medicine

DOI:
[10.1053/j.semnuclmed.2022.04.004](https://doi.org/10.1053/j.semnuclmed.2022.04.004)

IMPORTANT NOTE: You are advised to consult the publisher's version (publisher's PDF) if you wish to cite from it. Please check the document version below.

Document Version
 Publisher's PDF, also known as Version of record

Publication date:
 2022

[Link to publication in University of Groningen/UMCG research database](#)

Citation for published version (APA):

Manafi-Farid, R., Askari, E., Shiri, I., Pirich, C., Asadi, M., Khateri, M., Zaidi, H., & Beheshti, M. (2022). [18F]FDG-PET/CT Radiomics and Artificial Intelligence in Lung Cancer: Technical Aspects and Potential Clinical Applications. *Seminars in Nuclear Medicine*, 52(6), 759-780. <https://doi.org/10.1053/j.semnuclmed.2022.04.004>

Copyright

Other than for strictly personal use, it is not permitted to download or to forward/distribute the text or part of it without the consent of the author(s) and/or copyright holder(s), unless the work is under an open content license (like Creative Commons).

The publication may also be distributed here under the terms of Article 25fa of the Dutch Copyright Act, indicated by the "Taverne" license. More information can be found on the University of Groningen website: <https://www.rug.nl/library/open-access/self-archiving-pure/taverne-amendment>.

Take-down policy

If you believe that this document breaches copyright please contact us providing details, and we will remove access to the work immediately and investigate your claim.

Downloaded from the University of Groningen/UMCG research database (Pure): <http://www.rug.nl/research/portal>. For technical reasons the number of authors shown on this cover page is limited to 10 maximum.



ELSEVIER



[¹⁸F]FDG-PET/CT Radiomics and Artificial Intelligence in Lung Cancer: Technical Aspects and Potential Clinical Applications

Reyhaneh Manafi-Farid, MD,* Emran Askari, MD,[†] Isaac Shiri, PhD,[‡] Christian Pirich, MD, PhD,[§] Mahboobeh Asadi, MSc,* Maziar Khateri, MSc,* Habib Zaidi, PhD,^{‡,||,¶,#} and Mohsen Beheshti, MD, FEBNM, FASNC[§]

Lung cancer is the second most common cancer and the leading cause of cancer-related death worldwide. Molecular imaging using [¹⁸F]fluorodeoxyglucose Positron Emission Tomography and/or Computed Tomography ([¹⁸F]FDG-PET/CT) plays an essential role in the diagnosis, evaluation of response to treatment, and prediction of outcomes. The images are evaluated using qualitative and conventional quantitative indices. However, there is far more information embedded in the images, which can be extracted by sophisticated algorithms. Recently, the concept of uncovering and analyzing the invisible data extracted from medical images, called radiomics, is gaining more attention. Currently, [¹⁸F]FDG-PET/CT radiomics is growingly evaluated in lung cancer to discover if it enhances the diagnostic performance or implication of [¹⁸F]FDG-PET/CT in the management of lung cancer. In this review, we provide a short overview of the technical aspects, as they are discussed in different articles of this special issue. We mainly focus on the diagnostic performance of the [¹⁸F]FDG-PET/CT-based radiomics and the role of artificial intelligence in non-small cell lung cancer, impacting the early detection, staging, prediction of tumor subtypes, biomarkers, and patient's outcomes.

Semin Nucl Med 52:759-780 © 2022 The Authors. Published by Elsevier Inc. This is an open access article under the CC BY-NC-ND license (<http://creativecommons.org/licenses/by-nc-nd/4.0/>)

Introduction

Lung cancer is the second most common cancer and the leading cause of cancer-related death.¹ Despite the decrease in mortality in recent decades,² it remains a public health issue.³ The early diagnosis of the localized disease, accurate staging, response assessment, and prognostication are of paramount importance, which highly influence the treatment strategies and prognosis.^{2, 4, 5}

[¹⁸F]fluorodeoxyglucose positron emission tomography and/or computed tomography ([¹⁸F]FDG-PET/CT) is the widely accepted method for the non-invasive evaluation of non-small cell lung cancer (NSCLC) in different clinical settings.⁵⁻⁸ However, some limitations hinder [¹⁸F]FDG-PET/CT from becoming the ideal method. For example, inflammatory reactions in the thoracic region may cause false-positive findings, and small lesions and micro metastasis may be overlooked.⁹ Therefore,

*Research Center for Nuclear Medicine, Shariati Hospital, Tehran University of Medical Sciences, Tehran, Iran.

[†]Department of Nuclear Medicine, School of Medicine, Mashhad University of Medical Sciences, Mashhad, Iran.

[‡]Division of Nuclear Medicine and Molecular Imaging, Geneva University Hospital, Geneva, Switzerland.

[§]Division of Molecular Imaging and Theranostics, Department of Nuclear Medicine, University Hospital Salzburg, Paracelsus Medical University, Salzburg, Austria.

^{||}Geneva University Neurocenter, Geneva University, Geneva, Switzerland.

[¶]Department of Nuclear Medicine and Molecular Imaging, University of Groningen, University Medical Center Groningen, Groningen, The Netherlands.

[#]Department of Nuclear Medicine, University of Southern Denmark, Odense, Denmark.

Address reprint requests to Mohsen Beheshti, MD, FEBNM, FASNC, Division of Molecular Imaging and Theranostics, Department of Nuclear Medicine & Endocrinology, University Hospital Salzburg, Paracelsus Medical University, Salzburg, Austria. E-mail: m.beheshti@salk.at

there is a need for improvement of the current imaging techniques to fulfil the clinical requirements.

[¹⁸F]FDG-PET/CT images are visually and semi-quantitatively evaluated for the clinical assessment. Nevertheless, it has been demonstrated that PET/CT images are not just photos. There are numerous other characteristics of the lesions and surrounding tissues, embedded in the images, which are imperceptible and are not calculated by the available practical software.¹⁰ These quantitative parameters, called features, can be extracted from the images and analyzed to predict different characteristics of the lesions. This process is known as radiomics, so-called the “more than meets the eye”¹¹.

Radiomics uses digital data to define morphology, intensity, texture, etc. of the lesions and then correlates them with clinical, histological, and molecular findings. Over the last decade, [¹⁸F]FDG-PET/CT radiomics has been applied to differentiate malignant solitary pulmonary nodules (SPN) from benign lesions and increase staging accuracy, as well as to predict histology, tumor biomarkers, response to therapy, and prognosis. It should be noted that the number of the extracted features is too much to be assessed by the statistical analysis methods; therefore, artificial intelligence (AI) and machine learning (ML) are exploited to produce more accurate predictive models. There are several technical factors, such as harmonized data sets, which may limit the optimal implementation of radiomics in the clinical setting.¹² To overcome these limitations, guidelines are developed for standardization,¹³ and also deep learning (DL) is increasingly employed to reduce some of the restrictions.¹² However, there is still a gap between the studies and the translation of radiomics into clinical practice.

Several studies have investigated the value of radiomics in different aspects of NSCLC. Only 1% of the radiomics studies priorly were performed in the field of nuclear medicine.¹⁴ Encouragingly, this has recently reached 16%, considering that radiomics-like studies were present in nuclear medicine even before the word of “radiomics” itself came to existence.¹² The main purpose of the current review is to provide an update on the recent status of [¹⁸F]FDG-PET/CT radiomics in the evaluation of NSCLC. First, we provide a brief review of the technical aspects. Afterwards, we summarize the recent studies assessing current applications of [¹⁸F]FDG-PET/CT

radiomics and AI in NSCLC and seek an answer for “Do radiomics and AI increase the diagnostic performance or implication of [¹⁸F]FDG PET/CT in the era of precision medicine?”

Technical Aspect of Radiomics

Radiomics and Artificial Intelligence

Radiomics is a process to convert conventional images to mineable data by extracting high dimensional quantitative semantic and/or agnostic features.¹⁵⁻¹⁸ Semantic features are defined as commonly used features for the region of interest (ROI) description by human observers.¹⁵⁻¹⁷ Agnostic features are those extracted by a computational process for ROI heterogeneity assessment. These features could be extracted using mathematical-based formula features (conventional radiomics features described by the image biomarker standardization initiative [IBSI]¹⁹) or deep convolutional neural network (CNN)-based features (extracted automatically through different convolutional layers).¹⁵⁻¹⁷ These features could be mine through the data mining process, employing different AI algorithms.²⁰ AI tries to mimic human behaviors and ML, as a subset of AI, consists of different algorithms enabling computers to do this task without explicit programming.^{21, 22} ML algorithms are mostly applied to extracted features (agnostic and/or semantic) with feature selection or dimensionally reduction and regression or classification steps. DL is a ML algorithm that performs not only all these ML steps (feature selection, dimensionally reduction, regression, or classification) but also features extraction in one package.²¹

Radiomics' Steps

Radiomics is a multidisciplinary (imaging technologist, medical physicist, radiologist, oncologist, statistician, computer scientist and data scientist) and multistep process, requiring different experts' collaboration.^{15-17, 23, 24} The standard radiomics process includes data acquisition, image reconstruction, image segmentation, image pre-processing, feature extraction, feature selection and ML, as well as model evaluation,²⁵ which we will discuss in following sections (Fig. 1).

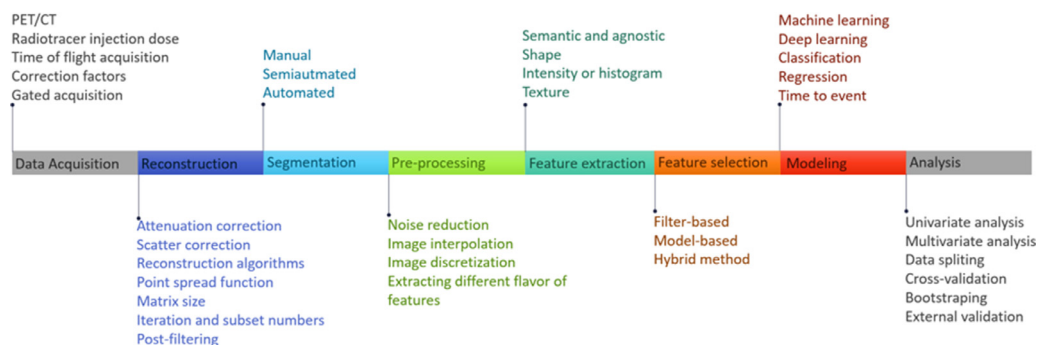


Figure 1 Multiple steps of radiomics, including PET/CT image data acquisition, image reconstruction with applying multiple correction steps, volume of interests' delineation, applying preprocessing and feature extraction, and machine learning steps (feature selection and classification/regression algorithm).

Data Acquisition

The image acquisition, the first step of radiomics study, is performed by technologists using different imaging modalities. Patients’ preparation and image acquisition should be performed in line with guidelines²⁶ for PET/CT imaging to provide high-quality images, enabling reproducible and repeatable radiomics study. For PET image acquisition, the radiotracer activity should be administered based on weight or body mass index. The CT part of PET/CT scanning is usually performed for attenuation and/or scatter correction and anatomical localization and correlation. Using these data, PET images will be reconstructed by different mathematical algorithms to provide standard images for quantitative assessment.²⁷ Different image artifacts^{28, 29} could arise during PET/CT image acquisition. These artifacts could be due to PET image itself, including image noise due to radiotracer injection or failure in the scatter correction process, which results in halo artifact in regions with high activity.^{28, 29} Some studies have addressed the image noise issue and employed advanced image processing using ML and DL to successfully decrease the image noise and increase the quality.³⁰⁻³⁶

Other artifacts could be due to CT, such as truncation and metal artifact, which could change the quantitative information of PET data.^{28, 29} Finally, the misregistration between PET and CT results in mis location of lesions, for example, those close to the liver dome.^{28, 29, 37} The impact of motion should be considered for the radiomics analysis of lung tumors.^{38, 39} Most recently, DL algorithms were proposed for direct attenuation and scatter corrections, bypassing the image reconstruction process with CT-based attenuation and scatter corrections, which potentially avoid or correct the mentioned artifacts.⁴⁰ Image acquisition in PET (injected dose, time-of-flight [TOF], and time per bed position) and CT [kVp, mAs, and pitch]) also impact on radiomics features. Proper values should be set to get high-quality images.²⁶ In addition, their impact should be considered for providing repeatable and reproducible radiomics studies in multi-scanner and multi-centric settings.^{41, 42}

Image Reconstruction

PET images could be reconstructed with different parameters, including reconstruction algorithm, TOF, point spread function, matrix size, iteration number, number of subsets and post-filtering.⁴³ Previous studies have shown that reconstructions’ parameters could highly affect radiomics reproducibility in different imaging modalities.⁴³⁻⁴⁷ These effects are feature dependent, and each parameter has a different impact on radiomics features.⁴³ Image reconstruction could be harmonized across different centers; however, different scanners from different providers have various sensitivity, which makes it infeasible to use the same set-up among imaging centers. Imaging data harmonization for different centers has been proposed to tackle this challenge, which is mentioned in the subsequent sections.

Image segmentation

Image segmentation is a crucial step for mathematical-based radiomic features extraction. Image segmentation could be

performed manually (by nuclear medicine physicians, radiologists, oncologists), semi-automated (set initial seed for segmentation followed by manual editing), and fully automated by DL algorithms.⁴⁸⁻⁵³ Different segmentations performed on the same tumors result in different values of radiomics features, and the reproducibility of these features should be assessed precisely.⁵⁴ Inter- and intra-observer variability and labor-intensive process of manual segmentation impede gathering large clean data sets for radiomic studies.⁵⁵ DL-based algorithms have been recently used in PET image segmentation to automatically delineate ROIs, which outperform conventional PET image segmentation algorithms.^{32, 48, 50-53}

Image pre-processing

Image pre-processing for radiomics analysis is performed for various reasons, including noise reduction, computationally efficient feature extraction, and extracting different flavor of radiomics features. The image interpolation to isotropic voxel size should be done to extract rotationally invariant texture features, which could be performed by up or down sampling.^{19, 56} Image discretization to fix bin number or fix bin width should be performed to normalize intensities; however, choosing the appropriate methods is an open question in radiomics studies.^{19, 56} Recently, some authors investigated the impact of these parameters on the reproducibility of PET image radiomics features⁵⁷⁻⁶⁰ and showed that fixed bin width results in reproducible features in PET images.⁵⁷

Various flavor of radiomics features could be extracted by using different filters, including wavelet (WL, applying either a high- or a low-pass filter in each of the three dimensions), Laplacian of Gaussian (LOG with different sigma values to extract fine, medium, and coarse texture), Exponential, Gradient, Logarithm, Square and Square Root scales for further radiomic investigation.

Feature extraction

Different types of features could be extracted from images, namely semantic and/or agnostic features.¹⁵ Semantic features are calculated by human observers describing ROI reporting different qualitative features that define the location, necrosis, spiculation and vascularity, etc. of tumors.¹⁵ Agnostic features are computed by mathematical-based formula description or deep CNN-based features. Mathematical-based radiomics features could be divided into shape-based, intensity and histogram-based, and texture features.^{19, 56} Texture features consist of second-order, such as gray level co-occurrence matrix (GLCM), and high-order, including gray level run length matrix (GLRLM), gray level dependence matrix (GLDM), gray level size zone matrix (GLSZM), and neighboring gray tone difference matrix (NGTDM).^{10, 19, 56} As these features could be calculated employing different formula, using IBSI features^{19, 56} is highly recommended to provide reproducible, and repeatable features. Different library and software such as Pyradiomics, SERA, LfEx, CERR, MITK, QIFE, CaPTk, RaCat, QuantImage, USZ, MIRP and QIFE have been evaluated for agreement with IBSI.^{19, 56} Deep CNN-based features are automatically extracted using different convolutional layers. They could be applied to

images for feature extraction; however, there is no guideline for optimal number and order of layers and it highly depends on developer and task.⁶¹

Feature Selection and Machine Learning Models

Large numbers of features could be extracted from ROIs; however, all these features are not informative for a specific task, and ML models (which perform classification, regression, or time to event task) would be highly prone to overfitting. Dimensionality reduction and feature selection could be performed in supervised (filter-based, model-based and hybrid), semi-supervised and unsupervised approaches. Different ML algorithms, including rule-based model, linear and nonlinear regression, neural networks, support vector, naïve bays and ensemble learning-based have been developed.⁶² These algorithms could be applied to features for classification (binary and multiclass classification), regression (ie, age prediction) and time to event prediction (survival analysis).^{63, 64} There is no “one fits all ML model ” for a specific task, ML models parameters and hyperparameters should be tuned based on task, and different ML models could be evaluated to reach the optimal ones.^{65, 66}

ML Model Evaluation

Radiomics models could be evaluated using different metrics (depending on the task) through different approaches.⁶⁷ These approaches include data splitting to train and/or validation and/or test sets, one-leave-out, cross validation, bootstrapping, one-leave-center-out (in case of multicentric study).⁶⁸ For the regression task, different metrics, including mean error (ME), mean absolute error (MAE), relative error (RE%), absolute relative error (ARE%), and normalized version of these metrics could be calculated. For time to event tasks, c-index and hazard ratio are the model parameter evaluation metrics.⁶⁹ For classification tasks, different metrics should be reported to assess models' performance, namely, accuracy, sensitivity, specificity, area under the receiver operating characteristic curve (AUC), positive predictive value (PPV), and negative predicted value (NPV).⁷⁰ For classification task different metrics should be reported to assess models performances, specifically in case of unbalance classes, NPV and PPV should be reported to assess power model in rare cases as we can get high accuracy and AUC but missing rare cases.⁷⁰ Using external validation set is highly recommended for model generalizability assessments.

Challenges and New Horizons

Different steps of radiomics such as image acquisition, reconstruction and segmentation could highly affect radiomics features value, resulting in non-repeatable and non-reproducible features. Different studies have evaluated the impact of these parameters on radiomics features' repeatability and reproducibility. Recently, harmonization approaches have been purposed in the feature domain (ie, ComBat) and image-level (ie, generative adversarial network) to tackle variability due to image acquisition, scanner, and reconstruction setting.⁷¹⁻⁷⁴

The imbalance class in radiomics studies is another challenge, which could potentially bias the model and still provide high accuracy but low specificity or low sensitivity (depending on the class) that may not be useful in the clinical practice.⁷⁵ Different approaches, such as data augmentation in image level or data sampling in features level have been proposed to address this issue.⁷⁵

Another subject is data sharing to build and evaluate a generalizable model due to legal and ethical problems.⁷⁶ Most recently, federated learning algorithms have been proposed to build models without sharing data. These approaches have been developed for two different tasks in PET imaging and could potentially expand in radiomics studies.^{77, 78} CT image information could be integrated into radiomics models in PET/CT studies using fusion in feature and fusion levels. Further studies could evaluate DL performance in PET/CT image fusion for radiomics models' improvement.^{71, 79-82}

Clinical Applications of [¹⁸F] FDG-PET/CT Radiomics in Non-Small Cell Lung Cancer

[¹⁸F]FDG-PET/CT is established as the standard imaging modality for the clinical management of NSCLC.⁵⁻⁸ However, there are still challenges for the interpretation of [¹⁸F] FDG-PET/CT images, especially for differentiation of inflammatory from cancerous tissues and for treatment monitoring of the novel targeted therapies.^{83, 84, 85} Therefore, technical and quantitative assisting tools are needed for improving the diagnostic performance of [¹⁸F]FDG-PET/CT in lung cancer for individualized disease management in different clinical scenarios, such as the early diagnosis, staging, prognostication, non-invasive evaluation of biomarkers and response assessment. To answer the clinical requirements, radiomics and AI are increasingly investigated in NSCLC in recent years. In the following sections, the value of [¹⁸F]FDG-PET/CT radiomics is discussed in different clinical settings.

Pulmonary Nodules

The prevalence of SPN in normal populations ranges from 2%-24%, which increases to 17%-53% in patients with risk factors of occult malignancy.⁸⁶ A non-negligible fraction of SPNs (ie, 1%-12%) harbors malignancy.⁸⁷ Owing to more employment of CT, especially in the COVID-19 era, guidelines have been developed to prevent unnecessary measures for SPNs.⁸⁸ A wide range of false-positive findings are detected on CT, leading to unavoidable harms,⁸⁹ and this is where radiomics comes to play.

There are multiple public SPN datasets to serve as a medium for radiomics surveys, of which the cancer imaging archive (TCIA) is one of the well-known repositories for [¹⁸F]FDG-PET/CT images.⁹⁰⁻⁹² Some studies have shown that radiomics using [¹⁸F]FDG-PET/CT are superior to CT for the estimation of malignancy in SPNs (AUCs for

conventional radiomics: 0.809-0.940 for [¹⁸F]FDG-PET/CT vs 0.646-0.908 for CT; and AUCs for DL: 0.877 for [¹⁸F]FDG-PET/CT vs 0.817 for CT).⁹³⁻⁹⁶ Interestingly, a recent multicentric prospective head-to-head comparison of these two modalities showed even more striking results. The AUCs for dynamic contrast-enhanced CT and [¹⁸F]FDG-PET/CT were 0.62 and 0.80, respectively, yet complementary to each other (combined AUC = 0.90).⁹⁷

Given the limited spatial resolution of [¹⁸F]FDG-PET/CT, small pulmonary nodules may not be detectable on [¹⁸F]FDG-PET and therefore, [¹⁸F]FDG-PET/CT is usually reserved for SPNs > 8 mm.⁸⁸ However, it seems that [¹⁸F]FDG-PET-derived radiomics features can be more sensitive (94% vs 58%) and accurate (93% vs 76%) than visual analysis for the detection of small lesions.⁹⁸ Moreover, emerging data suggest that ML can be helpful to reduce the noise, scan time, injected activity, and reconstruction time without a meaningful drop in the AUCs.^{33, 99} Also, DL approaches using newer image reconstruction methods may impact the diagnosis of small SPNs.¹⁰⁰

The inherent nature of [¹⁸F]FDG-PET/CT leads to well-known false-positive findings, interfering with the diagnosis of lung cancer.¹⁰¹ This challenge has been addressed by radiomics studies trying to reduce the false-positive rate. Radiomics can more accurately differentiate benign inflammatory lesions, such as tuberculosis (AUC = 0.889-0.93),¹⁰²⁻¹⁰⁴ pneumonia (accuracy = 82.5%),¹⁰⁵ and radiation pneumonitis (accuracy = 85%)¹⁰⁶ from lung cancer.^{84, 107} Also, some studies using texture analysis have suggested a possible added benefit of dual time-point imaging to further enhance the AUCs of radiomics (from 0.52-0.75 to 0.63-0.87).^{108, 109} A nomogram has also been developed using [¹⁸F]FDG-PET/CT radiomics combined with manual diagnosis, which has decreased the false-positive rate of manual diagnosis by 21.5% (AUC = 0.92).¹⁰⁴ Moreover, CNN method has shown a 93% reduction in false-positive results with a cost of 7% reduction in the sensitivity.¹¹⁰ On the other hand, some studies have shown that radiomics-based nomograms using conventional radiomics did not outperform nuclear medicine experts in the validation cohort, while DL algorithms marginally surpassed physicians.^{103, 111}

In a study to differentiate tuberculosis from lung adenocarcinoma, Hu et al. showed that the radiomics model outperformed the clinical model with marginal inferiority to the combined model (AUCs of 0.889, 0.644 and 0.909, respectively).¹⁰² Another study demonstrated insignificantly lower, yet complementary, performance of [¹⁸F]FDG-PET- compared to CT-based features for differentiation of tuberculosis from lung cancer (AUC: 0.91 vs 0.85, $P = 0.1554$).¹⁰³

The summary of the studies is provided in [Table 1](#). Although there are potential benefits for the prediction of malignancy in SPNs, there are some drawbacks,¹¹² and AI is still immature in this field to be clinically applied. In fact, a comprehensive review revealed that most radiomics studies in this domain lack relevant comparator or independent and/or external validation of the models.¹¹³ Also, for ML, 3D approaches still suffer from sufficient sample size for such purposes.¹¹⁴⁻¹¹⁶ Noteworthy, along with the ability of

automatic detection, DL algorithms seem to have higher discriminative power, possibly due to bypassing the segmentation and considering the tumor surrounding and whole-body data. Future studies should focus on the algorithms of DL combined with clinical information to increase the diagnostic performance of AI in the detection of nodules and differentiation of malignant from benign lesions.

Histologic Subtype Differentiation

Given the invasive nature of tissue biopsy, inadequacy and/or non-feasibility of sampling in some cases, and also the unmet need to differentiate the pathologic subtypes for treatment planning, radiomics come to play for the non-invasive differentiation of the histologic tumor subtypes.¹¹⁷

In this regard, different studies have shown a discriminative role for radiomics and ML models.^{118, 119} [Table 2](#) provides the summary of the investigations. Early radiomics studies pointed out that texture features had a role in distinguishing adenocarcinoma (ADC) from Squamous cell carcinoma (SqCC).¹¹⁹ Some authors showed that [¹⁸F]FDG-PET radiomics features and ML models outperformed those of CT (AUC: 0.80-0.83 vs 0.69-0.79).^{120, 121} Also, DL methods have been employed, showing superiority over conventional radiomics for differentiation of ADC from SqCC (AUC: 0.841 vs 0.794).¹¹⁷

Additionally, some authors implemented clinical factors in the prediction models, demonstrating the additive value of combined models over radiomics-only models (AUCs of 0.78-0.98 vs 0.70-0.94).¹²¹⁻¹²³ Ren et al. showed that the model based on both clinical factors and tumor markers is superior to imaging-based models for discrimination of subtypes; however, the combined model had a higher AUC of 0.90.¹²¹

There are also some efforts to differentiate primary and metastatic lung lesions using radiomics (AUC: 0.61-0.97).^{120, 124} Again, [¹⁸F]FDG-PET-based radiomics were superior to CT-based features (AUC: 0.57 vs 0.88).¹²⁰ A hybrid approach using ML models could optimally classify primary and metastatic lung lesions using [¹⁸F]FDG-PET (AUC = 0.983) and CT (AUC = 0.828).¹²⁵ Another study showed that fused signature combining [¹⁸F]FDG-PET/CT and clinical findings achieved the highest diagnostic accuracy (AUC = 0.953).¹²⁶ Moreover, the ComBat harmonization method has been applied to multicenter data, improving the predictive performance of PET and fused PET/CT models.⁸²

Overall, the [¹⁸F]FDG-PET/CT-based radiomics seem promising for the differentiation of tumor subtypes, especially using DL and implementing clinical factors in the prediction models. The non-invasive evaluation is of particular importance in patients with large or unresectable lesions or those with known other malignancies. Apparently, due to higher prevalence, most studies have focused on ADC and SqCC. Differentiating other subtypes is also worth investigating in future studies using multiclass classification ML algorithms.

Table 1 Summary of Studies Evaluating the Discriminative Power of Radiomics and Artificial Intelligence in Predicting the Nature of Pulmonary Nodules

| Author | Year | Pt No. | Aim | Reference standard | Segmentation method | Classifier | Dataset classification* | Result |
|-------------------------|------|-----------|---|------------------------|--------------------------|----------------------|----------------------------------|-----------------------|
| Chen ¹⁰⁷ | 2017 | 85 | Malignant vs Benign | Pathology or follow-up | Manual | ML | Resampling - type 1b | AUC = 0.91 |
| Guo ¹⁰⁶ | 2017 | 40 | Discrimination of lung cancer from pneumonia | - | Manual | ML | - | Accuracy = 85% |
| Suga ²³⁸ | 2021 | 63 | Discrimination of lung cancer from pneumonia | Pathology | Semiautomatic | Statistical analysis | One dataset - type 1a | AUC = 0.82-0.83 |
| Watanabe ¹⁰⁵ | 2018 | 20 | Discrimination of lung cancer from pneumonia | Pathology or follow-up | Semiautomatic | ML | - | Accuracy = 82.5% |
| Wu ¹¹⁵ | 2018 | 2,789,675 | Malignant vs Benign | - | - | ML | - | Accuracy = 77% |
| Chen ¹⁰⁸ | 2019 | 116 | Malignant vs Benign | Pathology or follow-up | Manual | Statistical analysis | Resampling - type 1b | AUC = 0.89 |
| Kang ¹⁰⁴ | 2019 | 268 | Reducing PET/CT false positive rate | Pathology or follow-up | Manual and Semiautomatic | ML | Random split-sample - type 2a | AUC = 0.98 |
| Nakajo ¹⁰⁹ | 2019 | 59 | Malignant vs Benign | Pathology | Manual and automatic | Statistical analysis | One dataset - type 1a | AUC = 0.98 |
| Zhang ⁹⁴ | 2019 | 135 | Malignant vs Benign | Pathology | Manual | ML | Resampling - type 1b | AUC = 0.887 |
| Hu ¹⁰² | 2020 | 235 | Malignant vs Benign | Pathology or follow-up | Semiautomatic | ML | Random split-sample - type 2a | AUC = 0.889 |
| Chen ⁸⁴ | 2021 | 317 | Malignant vs Benign | Pathology | Semiautomatic | ML | Random split-sample - type 1b | AUC = 0.727 |
| Du ¹⁰³ | 2021 | 174 | Malignant vs Benign | Pathology | Manual | ML | Random split-sample - type 2a | AUC = 0.93 |
| Park ⁹⁵ | 2021 | 359 | Malignant vs Benign | Pathology | - | DL | - | AUC = 0.837 and 0.877 |
| Shao ¹¹⁴ | 2021 | 106 | Malignant vs Benign | Pathology or follow-up | Semiautomatic | DL | Resampling - type 1b | AUC = 0.97 |
| Zhou ¹²⁵ | 2021 | 769 | Discrimination of lung cancer from metastasis | Pathology | Semiautomatic | ML | Random split-sample - type 1b/2a | AUC = 0.983 |
| Zhang ¹¹¹ | 2022 | 174 | Malignant vs Benign | Pathology | Manual | DL/ ML | Resampling - type 1b | AUC = 0.84 |

AUC, Area under curve; DL, Deep learning; ML, Machine learning; PET/CT, Positron emission tomography/computed tomography; Pt No., Number of patients.

All studies were retrospective.

*Based on TRIPOD (transparent reporting of a multivariable prediction model for individual prognosis or diagnosis) classification.

Table 2 The Summary of Studies Differentiating the Histologic Subtypes of Non-Small Cell Lung Cancer Using Radiomics and Artificial Intelligence

| Author | Year | Pt No. | Aim | Reference standard | Segmentation method | Classifier | Dataset Classification* | Results |
|-------------------------|------|--------|--|--------------------|---------------------|------------|--|--------------------|
| Ma ¹¹⁹ | 2018 | 341 | Differentiation of subtypes | Pathology | Manual | ML | Resampling - type 1b | AUC = 0.89 |
| Kirienko ¹²⁰ | 2018 | 534 | Differentiation between primary and metastatic lung lesions | Pathology | Semiautomatic | ML | Random split-sample - type 2a | AUC = 0.91 |
| Li ¹²⁶ | 2018 | 207 | Classification of pulmonary nodules/ Predicting histological subtypes | Pathology | - | ML | Resampling - type 1b | AUC ≥ 0.907 |
| Sha ¹²³ | 2019 | 100 | Differentiation of subtypes | Pathology | Manual | ML | Temporal external validation - type 2b | AUC = 0.781 |
| Han ¹¹⁷ | 2021 | 1419 | Differentiation of subtypes | Pathology | Semiautomatic | ML, DL | Random split-sample - type 2a | AUC= 0.903 |
| Koyasu ¹¹⁸ | 2020 | 188 | Differentiation of subtypes | Pathology | Manual | ML | - | AUC= 0.843 |
| Yan ¹²⁴ | 2020 | 445 | Differentiation of subtypes and primary and metastatic lung lesions | Pathology | Automatic | ML | Random split-sample 1b/2a | AUC= 0.98 and 0.99 |
| Zhou ¹²⁵ | 2021 | 769 | Differentiation of subtypes | Pathology | Semiautomatic | ML | Random split-sample - type 1b/2a | AUC = 0.897 |
| Ren ¹²¹ | 2021 | 315 | Differentiation of subtypes | Pathology | Manual | ML | Random split-sample - type 2a | AUC= 0.90 |
| Ji ¹²² | 2021 | 253 | Differentiation of subtypes | Pathology | Semiautomatic | ML | Temporal external validation - Type 2b | AUC= 0.978-0.989 |

AUC, Area under curve; DL, Deep learning; ML, Machine learning; Pt No., Number of patients. All studies are retrospective.

*Based on TRIPOD (transparent reporting of a multivariable prediction model for individual prognosis or diagnosis) classification.

Table 3 Summary of Studies Evaluating the Staging in Non-Small Cell Lung Cancer Patients Using Radiomics and Artificial Intelligence

| Author | Year | Pt. No. | Aim | Reference standard | Segmentation method | Classifier | Dataset Classification* | Results |
|-------------------------|------|---------|-------------------------|-----------------------------------|--------------------------|----------------------|---|---------------------------------|
| Gao ¹⁴⁴ | 2015 | 132 | LN-staging | Pathology | Manual | ML | Random split-sample - type 2a | AUC = 0.689 |
| Coroller ¹⁵⁸ | 2016 | 108 | Prediction of DM | - | - | - | - | AUC = 0.64 |
| Wu ¹⁵⁹ | 2016 | 101 | Prediction of DM | Pathology | Semiautomatic | ML | Temporal external validation - Type 2b | AUC = 0.80 |
| Kirienko ¹³⁰ | 2017 | 31 | LN-staging | Pathology | Semiautomatic | Statistical analysis | One dataset - type 1a | For some features: p>0.05 |
| Wang ¹⁴⁶ | 2017 | 168 | LN-staging | Imaging and pathology | Manual | ML, DL | Resampling - type 1b | AUC = 0.91 |
| Kirienko ¹³¹ | 2018 | 472 | T-staging | Imaging and pathology | Semiautomatic | DL | Random split-sample - type 2a | AUC = 0.68 |
| Lyu ¹⁵³ | 2020 | 130 | LN-staging | Pathology | - | ML | - | AUC = 0.917 |
| Tau ¹⁵² | 2020 | 264 | Prediction of LN and DM | Imaging, pathology, and follow-up | Semiautomatic and manual | DL | Resampling - type 1b | LN: AUC = 0.8 DM: AUC = 0.65 |
| Chang ¹⁴⁹ | 2021 | 528 | LN-staging | Pathology | Manual | ML | Random split-sample - type 2a | AUC = 0.94 |
| Taralli ¹⁴⁸ | 2021 | 540 | LN-staging | Pathology | Semiautomatic | DL | Resampling - type 1b | AUC = 0.769 |
| Wallis ¹⁵⁴ | 2021 | 125 | LN-staging | Pathology | Semiautomatic | DL | Different scanner external validation - type 2b | Sensitivity = 0.88 |
| Yoo ¹⁴⁷ | 2021 | 980 | LN-staging | Pathology | Semiautomatic | ML | Resampling - type 1b | AUC = 0.85 |
| Zheng ¹⁴⁵ | 2021 | 716 | LN-staging | Pathology | Manual | ML | Split-sample - type 2a | AUC = 0.80 |

AUC, Area Under Curve; DL, Deep learning; DM, Distant metastasis; LN, Lymph node; ML, Machine learning; Pt No., Number of patients. All studies were retrospective.

*Based on TRIPOD (transparent reporting of a multivariable prediction model for individual prognosis or diagnosis) classification.

Staging

T-staging

T-staging is usually performed using CT,^{101, 127, 128} and can be improved by [¹⁸F]FDG-PET data (Table 3).^{101, 128, 129} A few studies in this subtopic exists for the role of [¹⁸F]FDG-PET/CT radiomics.^{130, 131} For example, Kirienko et al. designed a CNN-based algorithm and classified NSCLC as T1/2 or T3/4 with an AUC of 0.68.¹³¹

N-staging

Lymph node (LN) staging is a crucial step for optimum treatment in NSCLC and is still a challenging issue. The current imaging modalities do not provide enough accuracy for this purpose, especially in endemic areas of granulomatous diseases.^{132, 133} The patient-based and node-based sensitivities of [¹⁸F]FDG-PET/CT are approximately 62%-67% with the specificities of about 87%-93%.^{134, 135} The corresponding values for diffusion-weighted magnetic resonance imaging are 72% and 97%, respectively.¹³⁵ Therefore, invasive pathologic evaluation is used for mediastinal N-staging with its inherent disadvantages.^{5, 136, 137} The discrimination of N0 and N1 disease is especially important when the standard surgery is not planned and the LNs are not dissected. Therefore, the additive value of radiomics is being evaluated in mediastinal N-staging.

Traditionally, the Hounsfield unit of CT and standardized uptake value (SUV) of [¹⁸F]FDG-PET are used to predict LN metastasis.^{134, 138} The use of ML-based classification in this subtopic roots back to before applying radiomics,¹³⁹ when simple metabolic parameters, such as SUV_{max}, were implemented in non-radiomics studies to build predictive ML models (AUCs: 0.886-0.962).¹⁴⁰⁻¹⁴² Moreover, some studies evaluated the CT-based radiomics and added only the SUV_{max} to the models to discover the additive value of metabolic parameters for N-staging (AUCs: combined = 0.838-0.872 vs CT = 0.822-0.828).^{9, 143} Although the models showed an acceptable predictive power, it was marginally higher than the accuracy of conventional parameters.⁹ The corresponding values were 0.73 for short-axis diameter ≥ 1.0 cm and 0.82 for SUV_{max} ≥ 2.5 .⁹

Using [¹⁸F]FDG-PET/CT radiomics, the reported accuracies for N-staging are rather wide. In an early study, ML was not superior to traditional SUV_{max} (0.652 vs 0.579-0.689, respectively).¹⁴⁴ However, in another study, the [¹⁸F]FDG-PET/CT-based model resulted in an AUC of 0.80 compared to 0.61 for physicians.¹⁴⁵ Also, Wang et al. claimed that the accuracy of CNN for N-staging is not significantly higher than that of assessed by experts (AUC = 0.91 and accuracy = 0.86 vs accuracy = 0.82).¹⁴⁶ It seems that AI models show higher sensitivity while physicians' reports have higher specificity with comparable accuracy for predicting histologic LN status.¹⁴⁶⁻¹⁴⁸ One of the interesting results of Yoo et al.'s study was that the sensitivity of ML was approximately twice higher than that of physicians in LNs with SUV_{max} < 3.5, but the specificity was still lower.¹⁴⁷

Some authors have incorporated the clinical information into [¹⁸F]FDG-PET/CT radiomics, reporting higher

performance for combined models.^{147, 149} Yoo et al. reported an AUC of 0.85 for the combined model vs 0.75 for physicians.¹⁴⁷

Patients with more hypermetabolic tumors have a higher chance of occult LN metastasis.^{150, 151} The radiomics of the primary tumor has also been evaluated to predict occult LN involvement, reaching an AUC of 0.78 with ML¹⁴⁵ and 0.80 with CNN¹⁵². Of interest, a model combining [¹⁸F]FDG-PET with breath-hold thin-slice chest CT achieved the AUC of 0.917 in stage I adenocarcinoma.¹⁵³

One of the main challenges is the robustness of the features or models using different acquisition systems or reconstruction methods. Wallis et al. used CNN to predict LN metastasis in the mediastinum.¹⁵⁴ They applied transfer learning to the second set of data obtained from another acquisition system, which increased the sensitivity from 0.53-0.88. However, the false-positive rate was also increased (from 0.24-0.69).¹⁵⁴

In summary (Table 3), there are limitations for the assessment of N-staging using [¹⁸F]FDG-PET/CT radiomics, such as the presence of reactive LNs or difficulty in histologic evaluation of each LN. The diagnostic performance of AI in the prediction of LN involvement seems only slightly higher than that of experts. In this regard, a recent systematic review studied the performance of the radiomics models for staging purposes.¹⁵⁵ The AUCs, sensitivities and specificities of the studies were 0.64-0.94, 52%-99%, and 60%-99%, respectively.¹⁵⁵ The authors concluded that heterogeneous study designs and lack of prospective validation in most studies preclude using radiomics for current clinical decisions.¹⁵⁵ Additionally, there are limitations for most studies, excluding small or inactive lesions, although the small size and low metabolism of the metastasis are the main challenges for N-staging. Future studies should focus on the role of automatic detection, DL, and combined models-incorporating all LN features, primary tumor characteristics and clinical information.

M-staging

Current imaging modalities can determine the M-stage with high accuracy.^{156, 157} Even though [¹⁸F]FDG-PET/CT is the modality of choice in this realm, with the exception of central nervous system metastasis, any suspicious foci of metastatic involvement should be ascertained by using additional imaging or biopsy.¹⁰¹ Radiomics has been implemented to also predict distant metastasis. In early radiomics studies, the features of the primary tumor barely predicted distant metastasis (AUC = 0.64-0.71).^{158, 159} Interestingly, even CNN did not improve the performance for prediction for distant metastasis at diagnosis (AUC = 0.71).¹⁵² Whether [¹⁸F]FDG-PET/CT radiomics may one day obviate the need for complementary imaging or biopsy is yet to be determined.

Prediction of Biomarkers

Lung cancer is a heterogeneous tumor,¹⁶⁰ and various responsible gene mutations have been detected so far.¹⁶⁰ Tumor genotype is translated into its phenotype. Evaluation

Table 4 Summary of Studies Evaluating the Prediction of Biomarkers in Non-Small Cell Lung Cancer Patients Using Radiomics and Artificial Intelligence

| Author | Year | Pt No. | Aim | Reference standard | Segmentation method | Classifier | Dataset classification* | Results |
|---------------------------|------|--------|---|---|--------------------------|----------------------|----------------------------------|---|
| Yip ¹⁷² | 2017 | 348 | Predicting EGFR and KRAS mutations | Genomic analysis | Semiautomatic | Statistical analysis | One dataset - type 1a | AUC = 0.67 and 0.54, retrospectively |
| Zhang ¹⁶⁷ | 2018 | 180 | Predicting EGFR mutation | Genomic analysis | Manual | ML | Split-sample | AUC = 0.8725 |
| Novikov ¹⁶² | 2019 | 84 | Prediction of tumor grade | Pathology | Semiautomatic | DL | Random split-sample - type 2a | Accuracy = 91- 100% |
| Moon ¹⁶⁴ | 2019 | 176 | Prediction of mutation burden | Genomic analysis | Semiautomatic | Statistical analysis | One dataset - type 1a | r = 0.592, p = 0.028 |
| Li ¹⁶⁸ | 2019 | 115 | Predicting EGFR mutation | Genomic analysis | Manual and Semiautomatic | ML | Resampling - type 1b | AUC = 0.805 |
| Moitra ¹⁸⁹ | 2019 | 211 | Automated grading | Histology | - | ML | Resampling - type 1b | AUC = 0.96 |
| Jiang ¹⁷⁸ | 2019 | 80 | Predicting EGFR mutation | Genomic analysis | Semiautomatic | ML | Resampling - type 1b | AUC = 0.953 |
| Mu ¹⁷⁷ | 2020 | 616 | Treatment guidance (TKI vs ICI) | Genomic analysis, follow-up and imaging | Semiautomatic | DL | External validation -type 3 | AUC = 0.81 |
| Zhang ¹⁶⁹ | 2020 | 248 | Predicting EGFR mutation | Genomic analysis | Semiautomatic | ML | Random split-sample - type 2a | AUC = 0.87 |
| Nair ¹⁷⁰ | 2020 | 50 | Predicting EGFR mutation/ Differentiating mutation exons | Genomic analysis | Manual | ML | Resampling - type 1b | AUC = 0.87 and 0.86, respectively |
| Shiri ¹⁷¹ | 2020 | 150 | Predicting EGFR and KRAS mutations | Genomic analysis | Semiautomatic | ML | Random split-sample - type 2a | AUC = 0.82 and 0.80, respectively |
| Shiri ⁷¹ | 2022 | 136 | Predicting EGFR and KRAS mutations | Genomic analysis | Semiautomatic | ML | Random split-sample - type 2a | AUC = 0.94 and 0.93, respectively |
| Sanduleanu ¹⁶³ | 2020 | 221 | Prediction of tumor hypoxia | Hypoxia-PET | Manual | ML | External validation -type 3 | AUC = 0.73 |
| Whi ¹⁷⁴ | 2020 | 64 | Predicting EGFR mutation | Genomic analysis | Manual | Statistical analysis | One dataset - type 1a | OR = 4.08-4.57 |
| Yang ¹⁸⁰ | 2020 | 174 | Predicting EGFR mutation/ Differentiating mutation exons | Genomic analysis | Semiautomatic | ML | Random split-sample - type 2a | AUC = 0.71 and 0.73, respectively |
| Jiang ¹⁸⁶ | 2020 | 399 | Predicting PD-L1 expression | IHC | Semiautomatic | ML | Random split-sample - type 2a | > 1%: AUC = 0.85-0.97 > 50%: AUC = 0.88-0.77 |
| Zhang ¹⁸² | 2020 | 173 | Predicting EGFR mutation/ Differentiating mutation exons | Genomic analysis | Manual and automatic | ML | Random split-sample - type 1b | AUC = 0.827 and 0.661, respectively |
| Liu ¹⁸¹ | 2020 | 148 | Predicting EGFR mutation | Genomic analysis | Manual | ML | Random split-sample - type 2a | AUC = 0.87 |
| Chang ¹⁷⁶ | 2021 | 583 | Predicting EGFR mutation | Genomic analysis | Semiautomatic and manual | ML | Random split-sample - type 1b/2a | AUC = 0.84 |
| Yin ¹⁷⁵ | 2021 | 301 | Predicting EGFR mutation | Genomic analysis | Manual | DL | Random split-sample - type 2a | AUC = 0.84 |
| Li ¹⁸⁴ | 2021 | 255 | Predicting PD-L1 expression | IHC | Semiautomatic | ML | Random split-sample - type 2a/1b | > 1%: AUC = 0.762 > 50%: AUC = 0.814 |
| Nie ¹⁴³ | 2021 | 272 | Predicting lymphovascular invasion | Histology | Semiautomatic | ML | External validation -type 3 | AUC= 0.838 |
| Chang ¹⁸⁷ | 2021 | 526 | Predicting ALK rearrangement status | IHC | Semiautomatic | ML | Random split-sample - type 2a | AUC= 0.88 |

ALK, Anaplastic lymphoma kinase; AUC, Area Under Curve; DL, Deep learning; EGFR, Epidermal growth factor receptor; ICI, Immune checkpoint inhibitor; IHC, Immunohistochemistry; KRAS, Kirsten rat sarcoma virus; ML, Machine learning; OR, Odds Ratio; PD-L1, Programmed death-ligand 1; PET, Positron emission tomography; Pt No., Number of patients; TKI, Tyrosine kinase inhibitor. All studies were retrospective.

*Based on TRIPOD (transparent reporting of a multivariable prediction model for individual prognosis or diagnosis) classification.

of mutations is becoming an inevitable step in the management of NSCLC,¹⁶¹ impacting the treatment options. Additionally, some features, such as tumor grade,¹⁶² lymphovascular invasion (LVI),⁴ or hypoxia,¹⁶³ influence the outcome. Therefore, predicting the presence of such biomarkers using the standard diagnostic imaging would be substantially advantageous, which is being investigated using [¹⁸F]FDG-PET/CT radiomics (Table 4).

A study failed to demonstrate a significant relation between radiomics features and the mutation burden.¹⁶⁴ The other showed modest relations between a number of mutations and [¹⁸F]FDG-PET/CT radiomics.¹⁶⁵ To begin with, mutations in epidermal growth factor receptor (EGFR) have a significant role in the development of NSCLC.¹⁶⁶ Those with EGFR mutation respond better to tyrosine kinase inhibitors (TKIs).¹⁶⁷ Therefore, the non-invasive prediction of EGFR mutation is tempting. Tumors with EGFR mutation tend to have more heterogeneity,^{168, 169} which might be captured by radiomics. Employing [¹⁸F]FDG-PET/CT conventional radiomics and ML for the prediction of EGFR mutation, a wide range of predictive power has been reported (AUC = 0.5–0.87), mostly around 0.75–0.80.^{168, 170–174} [¹⁸F]FDG-PET/CT-based features seemed superior over CT and PET-only radiomics (AUC = 0.80–0.84, 0.67–0.72, and 0.74–0.79, respectively).^{168, 175} Also, ML models outperformed conventional factors (AUCs = 0.82 vs 0.75).¹⁷¹

To further improve the accuracy, a number of scholars added clinical data in the predictive models, showing that the combined models (AUC = 0.82–0.87) surpassed imaging-based models (AUC = 0.68–0.77)^{168, 169, 176} and the clinical model alone (AUC = 0.69).¹⁶⁹ However, the accuracies of DL and DL plus clinical data were similar in another survey (AUC = 0.81 vs 0.84).¹⁷⁷ Moreover, in a study, [¹⁸F]FDG-PET/CT data combined with visual features of the images yielded a high AUC of 0.953.¹⁷⁸ In an attempt to increase performance, Shiri et al. applied feature harmonization, which proved to be feature-dependent, and slightly increased AUC for the prediction of EGFR mutation in different image modality including PET, CT and fused PET/CT image using ML algorithm (AUC increased from 0.87–0.90 to 0.92–0.94).⁷¹

There are two major EGFR mutations, 19DEL and 21L858R, which influence outcome and treatment options.¹⁷⁹ In this regard, [¹⁸F]FDG-PET/CT radiomics may discriminate 19DEL from 21L858R (AUC of 0.73–0.87).^{170, 180} Liu et al. predicted the presence of 19DEL and 21L858R with AUC of 0.77 and 0.92, respectively.¹⁸¹ On the other hand, Zhang et al. incorporated clinical information in the predictive model and reported that only one [¹⁸F]FDG-PET-based feature could differentiate 19DEL from 21L858R mutation with low predictive potential (AUC = 0.66).¹⁸²

Kirsten rat sarcoma viral (KRAS) also plays a significant role in NSCLC.¹⁶⁶ The predictive role of radiomics for KRAS mutation status is controversial. None of the [¹⁸F]FDG-PET-based features predicted KRAS mutation in a study by Yip et al.¹⁷² However, Shiri et al. demonstrated that a few features are predictive for KRAS mutation (AUC = 0.71).¹⁷¹ Also, they reported that the best model for predicting KRAS

mutation is the CT-based ML model.¹⁷¹ In a most recent study by Shiri et al. AUCs of 0.91–0.94 were reported for KRAS mutation classification using harmonized PET/CT fused image.⁷¹

The level of programmed death-ligand 1 (PD-L1) expression is an important factor for choosing immunotherapy in NSCLC.¹⁸³ The potential of radiomics to predict PD-L1 expression status is evaluated in a few studies. The PD-L1 expression levels >1% and >50% were predicted with AUCs of 0.762 and 0.814, respectively.¹⁸⁴ Similarly, Zhou et al. assessed tumor microenvironment immune types (ie, a combination of PD-L1 and CD8+ expression) and reached similar results with AUCs of 0.794, 0.699 and 0.811 for [¹⁸F]FDG-PET/CT-radiomics, clinical and combined models, respectively.¹⁸⁵ However, Jiang et al., showed that CT-derived models (AUC 0.80–0.97) are superior to [¹⁸F]FDG-PET-based models (0.61–0.75) for the prediction of PD-L1 expression.¹⁸⁶

Anaplastic lymphoma kinase (ALK) inhibitors are also used for the treatment of NSCLC patients with ALK rearrangement or positive for ROS1 (c-ros oncogene 1) or RET (rearranged during transfection) fusion.^{187, 188} Change et al. employed radiomics to predict ALK mutation status and reported that [¹⁸F]FDG-PET/CT radiomics predicted ALK mutation with an AUC of 0.86.¹⁸⁷ The result was comparable with the model based on combined [¹⁸F]FDG-PET/CT plus clinical data (AUC = 0.88).¹⁸⁷ The predictive features were more selected from CT features, possibly due to the higher resolution of CT compared to PET (1 mm vs 5 mm).¹⁸⁷ Moreover, Yoon et al. distinguished ALK, ROS1, or RET fusion-positive NSCLC from fusion-negative tumors with sensitivity and specificity of 73% and 70%, respectively.¹⁸⁸

Higher tumor grade¹⁶² and LVI⁴ are associated with a poorer prognosis. Novikov et al. employed radiomics-based models using different segmentation methods to predict tumor grade.¹⁶² None of the individual features were predictive.¹⁶² However, incorporating all features in predictive models, all three tumor grades were discriminated with overall accuracies of 71 to 100%.¹⁶² Also, Moitra et al. reported that fuzzy-rough nearest neighbor classifier, among other ML methods, provides higher performance for grading.¹⁸⁹ Moreover, Nie and colleagues could predict LVI using imaging-based features, with the CT-based radiomics plus SUV_{max} providing the highest AUC (0.79).¹⁴³

The proliferation rate is another prognostic factor in NSCLC.¹⁹⁰ In this regard, Palumbo et al. evaluated SUV_{max} and diameter of lesions on [¹⁸F]FDG-PET/CT images and applied ML to predict Ki-67 index, showing that the combination of SUV_{max} and lesion diameter could predict Ki-67 of > 25% with an accuracy of 82%.¹⁹⁰

Hypoxia is another biomarker which causes resistance to treatment in NSCLC. Sanduleanu et al. predicted hypoxic fraction > 20% using PET and CT-derived radiomics with AUC of 0.71–0.82 in both lung and head and neck cancers.¹⁶³

All in all, there is a plethora of factors and biomarkers impacting NSCLC patients' outcomes. Radiomics seems to predict EGFR mutation with acceptable but not ideal

accuracy. However, the primary results regarding KRAS mutation status are less favorable. Except for EGFR and KRAS mutations, other biomarkers have been evaluated in only a handful of studies. Radiomics in this field is rather unexplored. Also, studies implementing DL are lacking, mainly because of size of available data. Considering the growing knowledge about the impact of different biomarkers on the outcome, the non-invasive evaluation of such factors would promote individualized treatment approaches. Noteworthy, to be able to compare the results of different studies, complying with the standardized immunohistochemistry techniques and radiomics reporting criteria is necessary for the evaluation of biomarkers.¹⁹¹ Future studies can shed light on the role of radiomics in the non-invasive evaluation of different biomarkers in NSCLC.

Prognosis and Outcome

Predicting the outcome is an essential step for the patients' management. Various prognostic factors, such as stage, biomarkers, etc., have been identified.¹⁹²⁻¹⁹⁶ Also, the conventional semi-quantitative metabolic parameters on [¹⁸F]FDG-PET/CT have shown prognostic value.¹⁹⁷⁻¹⁹⁹ It is crucial to detect patients with a higher probability of recurrence who may benefit from more aggressive local or systemic treatments.²⁰⁰ The role of radiomics have also been investigated in this scenario (Table 5).

Early studies pointed out the inverse relation between tumor heterogeneity and overall survival (OS).²⁰¹ For example, in a study, the reduced heterogeneity was associated with a response to erlotinib.²⁰² Also, texture features such as entropy, dissimilarity, coarseness, contrast, and busyness were predictors of outcome in patients undergoing radiation therapy (RT) or chemoradiotherapy.²⁰³⁻²⁰⁶ Others found Asphericity to be a predictor of outcome.²⁰⁷ These features had additional prognostic value to metabolic tumor volumes (MTVs) and/or clinical variables.²⁰⁸⁻²¹⁰ Later, radiomics-based models were successfully developed to predict more outcome measures, namely OS, disease-specific survival and regional control.²¹¹

Attempts to predict OS or progression-free survival (PFS) using textural features showed promising results (AUCs = 0.665-0.762).²¹² The majority of studies showed an additive prognostic value of radiomics to clinical risk factors.^{124, 213} Even in some studies, radiomics features outperformed the combined clinical and radiomics data (AUCs of 0.68-0.75 vs 0.61-0.65).²¹⁴ Also, combined PET/CT models seem superior to each modality alone.⁷⁹⁻⁸¹ In contrast, some studies have reported that radiomics features were incapable of predicting PFS in patients undergoing curative RT,²¹⁵ and some have questioned the independent prognostic value of [¹⁸F]FDG-PET only images.²¹⁶

Surgery

Surgery is the treatment of choice in stage I/II NSCLC,^{5, 217} and some patients with stage IIIA disease or even some cases with oligometastasis.^{5, 218} However, 30%-55% of patients experience local/distant recurrence after curative surgery.²¹⁹

The value of [¹⁸F]FDG-PET/CT textural features for better stratification of the patients undergoing surgery has been addressed in a number of studies.²²⁰⁻²²²

Ahn et al. assessed the value of [¹⁸F]FDG-PET/CT radiomics for the prediction of disease-free survival (DFS) in patients undergoing surgery.²²³ They predicted recurrence with AUCs of 0.871-0.956 using ML.²²³ However, the clinical stage was a more powerful factor for the prediction of DFS.²²³ Kirienko et al. showed that the AUC of the CT-based model was higher than that of [¹⁸F]FDG-PET (0.75 vs 0.68).²¹⁴ Unexpectedly, the AUCs dropped after consideration of clinical findings (0.61 vs 0.65).²¹⁴ Using two different scanners and the lack of some important clinical data limited their study.²¹⁴ On the other hand, Christie et al. added clinical stage to [¹⁸F]FDG-PET/CT radiomics model and achieved an AUC of 0.79.²²⁴

"Extracting more information from medical images" needs one to think creatively and outside of the box.²²⁵ Radiomics studies usually focus on the target lesion while capturing more data from the penumbra and/or peritumoral area or even outside the tumor boundaries may provide additional information of prognostic significance.²²⁶ For example, Mattonen et al. evaluated the peritumoral region radiomics to predict recurrence and/or progression.²⁰⁰ The clinical stage was the best predictor of recurrence and/or progression (AUC = 0.68).²⁰⁰ However, adding MTV to peritumoral data empowered the predictive model (AUC = 0.74).²⁰⁰ Also, further addition of bone marrow uptake radiomics improved performance (AUC = 0.78).²²⁷ Others have tried to predict cachexia as an independent prognostic factor.²²⁸ This kind of approach to radiomics highlights the need for an interdisciplinary approach, an essential requirement for radiomics studies.²²⁹

Radiation Therapy

RT is another treatment option for NSCLC patients.^{5, 230} Unfortunately, no universal model beyond staging exists for prognostication of patients undergoing RT.²³⁰ Radiomics and pattern recognition using textural features may have a role to address the need for prediction of local recurrence, nodal failure or distant metastasis following RT.

In an early study, tumor- and LN-conventional features were used to predict recurrence after RT; however, the study failed to show a significant predictive power for local recurrence, tumor and LN features predicted overall recurrence (AUC = 0.69).²³¹ Li et al. predicted OS and nodal failure (AUCs = 0.64 and 0.66, respectively).²³² Furthermore, Oikonomou et al. showed the superiority of [¹⁸F]FDG-PET/CT radiomics over simple SUV_{max} measurements for the prediction of OS and recurrence.²¹¹ The performance was also improved involving clinical information (AUC = 0.97),²³³ as well as genetic and follow-up data (AUC = 0.79) during therapy (known as delta features).²³⁴

For distant metastasis prediction, radiomics studies showed the additive role of radiomics to the simple imaging or clinical parameters.^{159, 235} Also, the ML model based on both [¹⁸F]FDG-PET and CT achieved higher AUC compared

Table 5 Summary of the Studies Evaluated the Prognostic Value of Radiomics and Artificial Intelligence in Non-Small Cell Lung Cancer Patients

| Author | Year | Pt No. | Aim (prediction of) | Treatment | Segmentation method | Classifier | Data classification* | Follow-up time (months) | Results |
|---------------------------|------|--------|--|---|--------------------------|----------------------|---|--|---|
| Tixier ²⁰¹ | 2014 | 102 | OS, recurrence-free survival | Surgery, RT, chemotherapy, combination therapy | Manual and automatic | Statistical analysis | One dataset - type 1a | 36.6 (Median) | Some features predicted survival with $p < 0.05$ |
| Nakajo ²²¹ | 2018 | 55 | OS | Surgery | Semiautomatic | Statistical analysis | One dataset - type 1a | 23 (Median) | Multivariate analysis: Stage HR = 1.62, IV HR = 6.19 |
| Harmon ²²² | 2019 | 64 | OS, PFS | Surgery | Semiautomatic | Statistical analysis | One dataset - type 1a | - | DFS: HR = 0.72 OS: HR = 0.65 AUC = 0.72 |
| Mattonen ²²⁷ | 2019 | 227 | DFS | Surgery | Manual and semiautomatic | ML | Temporal split-sample - type 2b | 41 (Median) | AUC = 0.74 |
| Mattonen ²⁰⁰ | 2019 | 291 | Time to recurrence/ progression | Surgery | Semiautomatic | ML | External validation - type 3 ⁺ | 32-50 (Median varies per dataset) | AUC = 0.74 |
| Christie ²²⁴ | 2021 | 135 | Recurrence | Surgery | Semiautomatic | ML | Split-sample - type 2 | - | AUC = 0.79 |
| Pyka ²⁰⁴ | 2015 | 45 | LR and DSS | SBRT | Semiautomatic | Statistical analysis | One dataset - type 1a | 21.4 (Median) | Entropy for LR AUC = 0.872/ HR of entropy for LR: 7.48/ none for OS HR for dissimilarity = DSS: 0.822 and DFS: 0.834 |
| Lovinfosse ²⁰³ | 2016 | 63 | OS, DFS, DSS | SBRT | Semiautomatic | Statistical analysis | One dataset - type 1a | 27.1 (Median) | HR for dissimilarity = DSS: 0.822 and DFS: 0.834 |
| Hao ²³⁷ | 2017 | 48 | Distant failure | SBRT | - | ML | Resampling - type 1b | 18 (Median) | AUC = 0.70 |
| Takeda ²⁰⁵ | 2017 | 26 | LC, OS, PFS | SBRT | Semiautomatic | Statistical analysis | One dataset - type 1a | 36 (Median) | AUC for HILAE for LC = 0.72 |
| Zhou ²³⁵ | 2017 | 52 | Distant failure | SBRT | Semiautomatic | ML | Resampling - type 1b | 18 (Median) | AUC = 0.87 |
| Li ²³⁶ | 2018 | 110 | Distant failure | SBRT | Semiautomatic | ML | Split-sample - type 2 | 18 (Median) | AUC = 0.74 |
| Li ²³² | 2018 | 100 | OS, Nodal failure | SBRT | Semiautomatic | ML | Resampling - type 1b | - | AUC = 0.640 and 0.664, respectively |
| Oikonomou ²¹¹ | 2018 | 150 | RC, disease control, RFP, DSS, and OS | SBRT | Manual | ML | Resampling - type 1b | 27 (Median) | Radiomics remained the only predictors of OS, DSS and RC. Accuracy = 0.91 |
| Dissaux ²³³ | 2020 | 87 | LC | SBRT | Semiautomatic | ML | External validation - type 3 | 21.1-25.5 (Median varies per dataset) | AUCs for prediction of response: contrast = 0.82 coarseness = 0.8 busyness = 0.72 |
| Cook ²⁰⁶ | 2013 | 53 | treatment response, OS, PFS, local PFS | Chemoradiotherapy | Manual | Statistical analysis | One dataset - type 1a | 21.2 (Median) | AUCs for prediction of response: contrast = 0.82 coarseness = 0.8 busyness = 0.72 |
| Apostolova ²⁰⁷ | 2014 | 60 | OS, PFS | Surgery ± (chemo) radiotherapy or chemoradiotherapy | Semiautomatic | Statistical analysis | One dataset - type 1a | 10.1 (Median) | PFS: asphericity (HR = 3.66) and solidity (HR = 2.11) OS: asphericity (HR = 3.19) |
| Fried ²⁰⁹ | 2015 | 195 | OS | Chemoradiotherapy | Semiautomatic | ML | Resampling - type 1b | > 1 years; for living patients = 37 (Median) | AUC = 0.62 |
| Li ²³¹ | 2015 | 25 | Local and overall relapse | Chemoradiotherapy | Manual | ML | Resampling - type 1b ⁺ | 26 (Median) | AUC = 0.69 |
| Ohri ²⁰⁸ | 2016 | 201 | OS | Chemoradiotherapy | Semiautomatic | ML | Resampling - type 1b | 24 | The optimal cut-points for MTV and SUV _{mean} were 93.3 cm ³ , 0.018, respectively. |
| Dong ²¹² | 2016 | 58 | OS, PFS | Chemoradiotherapy | Semiautomatic | Statistical analysis | One dataset - type 1a | 60 (Median) | PFS: HR = 0.476, OS: HR = 0.519 |
| Kirienko ²¹⁴ | 2017 | 295 | DFS | RT or chemotherapy | Semiautomatic | Statistical analysis | Random split-sample | 20.1-20.5 (for CT or PET dataset, Median) | AUC = 0.68 |
| Luo ²³⁴ | 2018 | 118 | LC and Radiation Pneumonitis | (Chemo)radiotherapy | - | ML | Temporal split-sample - type 2b | 61-65 (Median varies per group) | AUCs for: pre-treatment = 0.77; During-treatment = 0.79 |
| Jensen ²¹⁰ | 2018 | 79 | OS | Chemoradiotherapy | Semiautomatic | ML | One dataset - type 1a | 22 (Median) | AUC = 0.739 |

Table 5 (Continued)

| Author | Year | Pt No. | Aim (prediction of) | Treatment | Segmentation method | Classifier | Data classification* | Follow-up time (months) | Results |
|-----------------------------|------|--------|--|-----------------------------|--------------------------|----------------------|--|---|---|
| Arshad ²⁴⁹ | 2019 | 358 | OS | (Chemo)radiotherapy | Semiautomatic | ML | Random and nonrandom split-sample - type 2 | 22 (Median) | HR = 1.61 |
| Krarup ²¹⁵ | 2019 | 233 | PFS | Chemoradiotherapy | Semiautomatic | ML | One dataset - type 1a | 631.5 days (Mean) | No radiomics features predicted PFS |
| van Timmeren ²⁴⁸ | 2019 | 138 | OS | (Chemo)radiotherapy | Manual | ML | Random split-sample - type 2a | 3.4-6.9 years (Median varies per dataset) | AUC ranged from 0.66 to 0.89 |
| Ahn ²²³ | 2019 | 93 | DFS | Surgery ± chemoradiotherapy | Semiautomatic | ML | Resampling - type 1b | 45 (Median) | AUC for RF = 0.956 |
| Astaraki ²⁵¹ | 2019 | 30 | OS | Chemoradiotherapy. | Semiautomatic | ML | Resampling - type 1b | 2 years | AUC = 0.90 |
| Konert ²¹⁶ | 2020 | 362 | OS | Chemoradiotherapy | Semiautomatic | ML | External validation - type 3 | 17-24 (Median varies per dataset) | AUC = 0.51 to 0.59 less than clinical model |
| Zhang ²⁴⁷ | 2020 | 82 | PFS | Chemoradiotherapy | Manual | ML | Random split-sample - type 2a | 1.9-2 years (Median varies per group) | AUC = 0.77-0.79 |
| Carles ²⁵² | 2021 | 48 | OS, LR, DM | Chemoradiotherapy | Manual and Semiautomatic | ML | External validation - type 3 [†] | - | AUC = 0.63 |
| Moran ²⁵⁰ | 2021 | 39 | OS | Chemoradiotherapy | - | Statistical analysis | - | - | AUC = 0.82-0.83 |
| Park ²⁶² | 2018 | 182 | PFS | TKI | Semiautomatic | ML | Split-sample | - | AUC = 0.662 |
| Mu ²⁵³ | 2020 | 194 | DCB, PFS, OS | ICI | Semiautomatic | ML | Temporal external validation - type 3 [†] | - | AUCs: DCB = 0.81 OS = 0.80 PFS = 0.77 AUCs = 0.74-0.88 |
| Park ²⁵⁹ | 2020 | 181 | CAS (marker for prediction of OS, PFS, treatment response) | ICI | Semiautomatic | DL | External validation - type 3 | - | AUCs = 0.74-0.88 |
| Valentinuzzi ²⁵⁷ | 2020 | 30 | Treatment response (OS > median of 14.9 months) | ICI | Semiautomatic | Statistical analysis | Resampling - type 1b | 21.4 (Median) | AUC = 0.90 |
| Polverari ²⁵⁶ | 2020 | 57 | Treatment response | ICI | Manual and semiautomatic | Statistical analysis | One dataset - type 1a | 10 (Median) | Association between several features with progressive disease |
| Mu ²⁵⁴ | 2021 | 697 | DCB, PFS, OS | ICI | Semiautomatic | DL | External validation - type 3 | - | AUC = 0.82 |
| Mu ²²⁸ | 2021 | 210 | Cachexia | ICI | Semiautomatic | ML | External validation - type 3 | 26 (Median) | AUCs ≥ 0.74 |
| Shao ²⁶³ | 2021 | 250 | PFS | TKI | Manual | ML | External validation - type 3 | >2 years | AUC = 0.60-0.71 |

AUC, Area under curve; CXR, Chest X-ray; CAS, Cytolytic activity score; DCB, Durable clinical benefit; DFS, Disease-free survival; DL, Deep learning; DM, Distant metastasis; DSS, Disease-specific survival; HILAE, High-intensity large-area emphasis; HR, Hazard ratio; ICI, Immune checkpoint inhibitor; LC, Local control; LR, Local recurrence; ML, Machine learning; OS, Overall survival; PFS, Progression-free survival; PET/CT, Positron emission tomography/computed tomography; Pt No., Number of patients; RC, Regional control; RFP, Recurrence-free probability; RT, Radiotherapy; SBRT, Stereotactic body radiation therapy; TKI, Tyrosine kinase inhibitor.

*Based on TRIPOD (transparent reporting of a multivariable prediction model for individual prognosis or diagnosis) classification.

[†]At least one cohort included prospectively gathered cases.

to either alone.²³⁶ Moreover, DL outperformed ML models for predicting distant disease.²³⁷

Differentiating radiation pneumonitis from residual/recurrent disease to avoid delay in treatment is a challenging issue after RT.²³⁸ These may have a similar appearance on CT.²³⁹⁻²⁴¹ Also, increased metabolism due to inflammation is common in [¹⁸F]FDG-PET/CT images,^{240, 242} which may decrease the accuracy of SUVs. To distinguish these two entities, Suga et al. showed that two conventional radiomics features outperformed SUV (AUC = 0.83-0.82 vs 0.63-0.64) but not MTV (AUC = 0.86).²³⁸

Chemoradiotherapy

Concurrent chemoradiotherapy is usually recommended for stage II LN-positive or stage III diseases.⁵ It may make patients prone to toxicity from intensive therapy without having a significant survival benefit.^{243, 244} For patients receiving chemoradiation, several factors are of prognostic significance.²⁴⁴⁻²⁴⁶ Yet, current clinical and imaging parameters are still imperfect in terms of prognostic power.²⁴⁴⁻²⁴⁶

The added value of radiomics signature to SUVs or clinical factors in NSCLC patients undergoing chemoradiation has been described (AUCs: 0.72-0.79)^{210, 247}. A study could not build a successful radiomics-based model.²⁴⁸ However, a multicenter study evaluated the pre-therapy [¹⁸F]FDG-PET/CT radiomics features for the prediction of survival in stage I-III NSCLC.²⁴⁹ The radiomics features-derived hazard ratio (HR) was 1.61 (CI 95%: 1.16-2.24), while SUV-related parameters were not predictive.²⁴⁹ Another smaller study emphasized the added value of combined [¹⁸F]FDG-PET radiomics with “conventional prognostic factors” to “conventional prognostic factors”-alone or CT radiomics for the prediction of OS (AUCs of 0.82, 0.68, and 0.62, respectively).²⁵⁰ Similarly, Astaraki et al. focused on a new partitioning method to predict OS. Their ML method outperformed conventional radiomics features (AUC = 0.90 vs. 0.71).²⁵¹ Using the changes in radiomics features (delta features) in the follow-up studies after chemoradiation, patients with increasing homogeneity in the primary tumor had a higher rate of local recurrence.²⁵²

Immunotherapy

Immune checkpoint inhibitors (ICIs) have an emerging role as consolidation therapy after chemoradiation in stage II/III NSCLC. They can also be employed with/without chemotherapy for the first-line treatment of metastatic patients.⁵ To predict response to ICIs, a study found a good AUC for [¹⁸F]FDG-PET/CT radiomics (0.81) and showed its additive value to the nomogram (AUCs of 0.77 and 0.80 for the prediction of OS and PFS, respectively).²⁵³ Furthermore, Mu et al. used DL and predicted PD-L1 expression status (AUC \geq 0.82), durable clinical benefit (AUC = 0.87), PFS (AUC = 0.77), and OS (AUC = 0.70).²⁵⁴

Following immunotherapy, pseudoprogression is likely, and imaging criteria may lag months to define the real progression warranting additional imaging.²⁵⁵ Radiomics may help predict the tumor response. Given that tumor heterogeneity can predict disease progression in these patients,²⁵⁶ a

study compared immunotherapy radiomics (so-called “iRADIOMICS”) with iRECIST (immunotherapy response evaluation criteria in solid tumors), showing a higher AUC for the prediction of response to treatment with pembrolizumab (0.90 vs 0.79-0.86).²⁵⁷

For the prediction of response to neoadjuvant immunotherapy in early-stage NSCLC, [¹⁸F]FDG-PET-derived radiomics features were uneventful in a study with small numbers of patients.²⁵⁸ However, employing tumor immune microenvironment, cytolytic activity score was predictive using [¹⁸F]FDG-PET/CT-based DL (AUCs = 0.74-0.88), which also correlated with PFS and OS.²⁵⁹ Also, responders to ICI were discriminated from non-responders ($P = 0.005$).²⁵⁹ Additionally, some authors tried to predict cachexia (as a factor for resistance to immunotherapy, AUC \geq 0.74)²²⁸ or severe immune-related adverse events (AUC = 0.88).²⁵³

Tyrosine Kinase Inhibitors

Adjuvant TKIs are reserved for stage IB-IIIa EGFR-mutated NSCLC.⁵ Simple measures such as SUV_{max} suffer from adequate diagnostic power for the prediction of EGFR status (summary ROC = 0.68).²⁶⁰ As discussed above, there is a possible role for [¹⁸F]FDG-PET/CT radiomics if the quality of the studies is further improved.²⁶¹ To predict outcome after treatment with TKI, some radiomics features and the changes in their values during therapy (delta features) predicted OS and response to TKI (erlotinib).²⁰² In another survey, pretreatment intratumoral heterogeneity was related to PFS after TKI treatment (gefitinib or erlotinib).²⁶² Also, radiomics predicted rapid progression after receiving TKI.²⁶³ Interestingly, the model based on radiomics showed better performance compared to the model combining radiomics with clinicopathologic data (AUCs: 0.76 vs 0.71) for the prediction of PFS.²⁶³ To evaluate the clinical benefit of DL in predicting EGFR mutation and its impact on treatment decision, Mu et al. reported that patients with high EGFR mutation signature have longer PFS when treated with TKIs while those with low EGFR mutation signature respond better to ICIs.¹⁷⁷

Discussion and Conclusion

An exponentially increasing number of studies are being published evaluating the role of AI in medical imaging. The preliminary results show that [¹⁸F]FDG-PET/CT-based radiomics provides additional valuable information in NSCLC patients.

To recapitulate, AI provides the possibility of automatic detection and also denoising and increasing the quality of studies with low-dose imaging, theoretically opening a horizon for screening of malignancies. In addition, radiomics may differentiate malignant pulmonary nodules and the subtypes of the primary lesions, especially when combined with clinical data, slightly better than physicians, moving one more step toward the non-invasive characterization of the lesions. The superiority of radiomics for the T- and M-staging has not been proved in the limited number of surveys.

Likewise, the prediction of LN involvement seems only slightly higher than that of experts. Additionally, the expanding field of biomarkers in oncology has been addressed. Most studies have shown promising potential for the prediction of EGFR mutation status, which may influence the decision for targeted therapies in the future. However, other biomarkers have scarcely been assessed. Moreover, it is crucial to predict the response to therapy in the early stages of treatment to timely adjust the management. In this regard, a large proportion of studies have reported the promising role of radiomics in predicting outcome as the endpoint of cancer management.

Nevertheless, the immediate physiological relevance of radiomics is not yet defined.²⁴⁹ A recent systematic review in this regard also concluded that the quality score of the studies is low, reflecting a lack of reproducibility.²⁶⁴ There are a few studies evaluating the prognostic value of [¹⁸F]FDG-PET/CT radiomics to predict outcomes after surgery or chemoradiation, showing a wide range of accuracies. There are known prognostic clinical factors. They should also be implemented in the predictive models to augment the predictive performance. Moreover, incorporating data from the peritumoral regions or even outside the tumor boundaries may provide additional prognostic information. Given the whole-body evaluation with DL, it may show higher performance in this regard. Also, there is a debate regarding the role of radiomics in prognostication after RT.²³⁹ Two recent systematic reviews addressed the utility of radiomics in this regard,^{230, 265} showing a modest predictive value for conventional radiomics for OS.²³⁰ However, DL seems more promising, which should be employed in future studies. These emerging pieces of evidence are expressed as a “significant potential” of radiomics in the recent EANM/SNMMI/ESTRO guidelines on the role of [¹⁸F]FDG-PET/CT in RT planning.²⁶⁶ Moreover, targeted therapies will have prominent roles in the management of NSCLC in future. Considering the costs and adverse events of targeted therapy, it is better to define which patients will have a durable clinical benefit. Incorporating radiomics may enhance the prognostic power of [¹⁸F]FDG-PET/CT and may impact the decision making. A comprehensive review on radiomics biomarkers in the field of immunotherapy is available, yet data on [¹⁸F]FDG-PET radiomics is not solid and warrants further improvement.²⁶⁷ Finally, delta features seem to possess prognostic significance in response evaluation. However, there are challenges in maintaining the consistency of parameters in different studies and robustness of the relevant features.

In conclusion, [¹⁸F]FDG-PET/CT radiomics seems to be advantageous for the evaluation of NSCLC in different settings. However, all fields suffer from shared drawbacks,^{112, 155, 191, 248, 261, 264, 267-270} i.e. standardized imaging, the method of radiomics implementation, and reporting, limit comparative studies and translation of radiomics into clinical practice. The repeatability and reproducibility of radiomics features should be assessed for robust radiomics modeling. Harmonization, data augmentation and federated learning algorithm could be employed to tackle acquisition/reconstruction variability, imbalance classes and data sharing

challenges in the clinic, respectively. Efforts have been made for standardization and improving the quality of reports, including the development of IBSI,¹³ TRIPOD (transparent reporting of a multivariable prediction model for individual prognosis or diagnosis)²⁷¹, and RQS (radiomics quality score)¹⁷, yet to be implemented in all published studies. Moreover, DL algorithms are increasingly employed and seemingly have equal or superior performance compared to conventional statistical analysis and ML models. Moreover, adding the clinical information into predictive models, mimicking the human decision approach, may improve the efficacy.

The wide implementation of AI in medical imaging research is to reach the unfulfilled dream of developing a rapid, one-step, diagnostic “machine.” It seems that there is still a long way to reach that goal. Also, whether virtual biopsy one day will become a reality remains to be answered.²⁷² However, by publishing standard reports, experts can use AI to improve their reports and enhance patients’ management. To accelerate the clinical use of radiomics, future studies should comply with the guidelines. Introducing the potential applications, advantages and limitations of AI in scientific meetings, seminars, and webinars would help increase awareness.

Funding

This research received no external funding.

Conflicts of Interest

The authors declare no conflicts of interest.

Acknowledgments

We wish to express our deep appreciation and gratitude to Milad Enferadi, Research Center for Nuclear Medicine, Shariati Hospital, Tehran University of Medical Sciences, for helping in literature search and providing the manuscripts.

References

1. Sung H, Ferlay J, Siegel RL, et al: Global cancer statistics 2020: GLOBOCAN estimates of incidence and mortality worldwide for 36 cancers in 185 countries. *CA Cancer J Clin* 71:209-249, 2021
2. National Cancer Institute: The Surveillance E, and End Results (SEER) Program. Cancer Stat Facts: Lung and Bronchus Cancer, 2021 Accessed December 11, 2011. Available at: <https://seer.cancer.gov/stat-facts/html/lungb.html>
3. Wong MCS, Lao XQ, Ho KF, et al: Incidence and mortality of lung cancer: Global trends and association with socioeconomic status. *Scientific Reports* 7:1-9, 2017.
4. Isaka M, Kojima H, Takahashi S, et al: Risk factors for local recurrence after lobectomy and lymph node dissection in patients with non-small cell lung cancer: Implications for adjuvant therapy. *Lung Cancer* 115:28-33, 2018
5. National Comprehensive Cancer Network: NCCN clinical practice guidelines in oncology (NCCN guidelines): Non-small cell lung cancer

- (Version 1.2022). 2021 Accessed December 08, 2021. Available at: https://www.nccn.org/professionals/physician_gls/pdf/nscl.pdf
6. Vansteenkiste J, Crinò L, Dooms C, et al: 2nd ESMO Consensus conference on lung cancer: Early-stage non-small-cell lung cancer consensus on diagnosis, treatment and follow-up. *Ann Oncol* 25:1462-1474, 2014
 7. Eberhardt WE, De Ruysscher D, Weder W, et al: 2nd ESMO Consensus conference in lung cancer: Locally advanced stage III non-small-cell lung cancer. *Ann Oncol* 26:1573-1588, 2015
 8. MacMahon H, Naidich DP, Goo JM, et al: Guidelines for management of incidental pulmonary nodules detected on CT Images: From the Fleischner Society 2017. *Radiology* 284:228-243, 2017
 9. Xie Y, Zhao H, Guo Y, et al: A PET/CT nomogram incorporating SUV-max and CT radiomics for preoperative nodal staging in non-small cell lung cancer. *Eur Radiol* 31:6030-6038, 2021
 10. Manafi-Farid R, Karamzade-Ziarati N, Vali R, et al: 2-[18F]FDG PET/CT radiomics in lung cancer: An overview of the technical aspect and its emerging role in management of the disease. *Methods* 188:84-97, 2021
 11. Hatt M, Tixier F, Visvikis D, et al: Radiomics in PET/CT: More Than Meets the Eye? *J Nucl Med* 58:365-366, 2017
 12. Hatt M, Cheze Le Rest C, Antonorsi N, et al: Radiomics in PET/CT: Current status and future AI-based evolutions. *Semin Nucl Med* 51:126-133, 2021
 13. The image biomarker standardisation initiative: Creative Commons Attribution 4.0 International License (CC-BY). 2022 Accessed 2022 Feb 09. Available at: <https://ibsi.readthedocs.io/en/latest/index.html>
 14. Limkin EJ, Sun R, Derclé L, et al: Promises and challenges for the implementation of computational medical imaging (radiomics) in oncology. *Ann Oncol* 28:1191-1206, 2017
 15. Gillies RJ, Kinahan PE, Hricak H: Radiomics: Images are more than pictures, they are data. *Radiology* 278:563-577, 2016
 16. Yip SS, Aerts HJ: Applications and limitations of radiomics. *Phys Med Biol* 61:R150-R166, 2016
 17. Lambin P, Leijenaar RTH, Deist TM, et al: Radiomics: the bridge between medical imaging and personalized medicine. *Nat Rev Clin Oncol* 14:749-762, 2017
 18. Saboury B, Rahmim A, Siegel E: PET and AI trajectories finally coming into alignment. *PET Clin* 16:xv-xvi, 2021
 19. Zwanenburg A, Vallières M, Abdalah MA, et al: The image biomarker standardization initiative: Standardized quantitative radiomics for high-throughput image-based phenotyping. *Radiology* 295:328-338, 2020
 20. Yousefirizi F, Pierre D, Amyar A, et al: AI-based detection, classification and prediction/prognosis in medical imaging: Towards radiophenomics. *PET Clin* 17:183-212, 2022
 21. LeCun Y, Bengio Y, Hinton G: Deep learning. *nature* 521:436-444, 2015
 22. Toosi A, Bottino AG, Saboury B, et al: A brief history of AI: How to prevent another winter (a critical review). *PET Clin* 16:449-469, 2021
 23. van Timmeren JE, Cester D, Tanadini-Lang S, et al: Radiomics in medical imaging: "how-to" guide and critical reflection. *Insights Imaging* 11:91, 2020
 24. Bouchareb Y, Moradi Khaniabadi P, Al Kindi F, et al: Artificial intelligence-driven assessment of radiological images for COVID-19. *Comput Biol Med* 136:104665, 2021
 25. Orhac F, Nioche C, Klyuzhin I, et al: Radiomics in PET imaging: A practical guide for newcomers. *PET Clin* 16:597-612, 2021
 26. Boellaard R, Delgado-Bolton R, Oyen WJ, et al: FDG PET/CT: EANM procedure guidelines for tumour imaging: version 2.0. *Eur J Nucl Med Mol Imaging* 42:328-354, 2015
 27. Zaidi H, Hasegawa B: Determination of the attenuation map in emission tomography. *J Nucl Med* 44:291-315, 2003
 28. Sureshbabu W, Mawlawi O: PET/CT imaging artifacts. *J Nucl Med Technol* 33:156-161, 2005. quiz 163-4
 29. Cook GJ, Wegner EA, Fogelman I: Pitfalls and artifacts in 18FDG PET and PET/CT oncologic imaging. *Semin Nucl Med* 34:122-133, 2004
 30. Sanaat A, Shooli H, Ferdowsi S, et al: DeepTOFSino: A deep learning model for synthesizing full-dose time-of-flight bin sinograms from their corresponding low-dose sinograms. *Neuroimage* 245:118697, 2021
 31. Nai Y, Schaefferkoetter JD, Fakhry-Darian D, et al: Improving lung lesion detection in low dose positron emission tomography images using machine learning presented at. In: 2018 IEEE Nuclear Science Symposium and Medical Imaging Conference, NSS/MIC 2018 - Proceedings, Institute of Electrical and Electronics Engineers Inc., 2018
 32. Schwyzer M, Ferraro DA, Muehlematter UJ, et al: Automated detection of lung cancer at ultralow dose PET/CT by deep neural networks – Initial results. *Lung Cancer* 126:170-173, 2018
 33. Nai YH, Schaefferkoetter J, Fakhry-Darian D, et al: Validation of low-dose lung cancer PET-CT protocol and PET image improvement using machine learning. *Phys Med* 81:285-294, 2021
 34. Cui J, Gong K, Guo N, et al: PET image denoising using unsupervised deep learning. *Eur J Nucl Med Mol Imaging* 46:2780-2789, 2019
 35. Ly J, Minarik D, Jögi J, et al: Post-reconstruction enhancement of [18F] FDG PET images with a convolutional neural network. *EJNMMI Res* 11, 2021
 36. Zhou L, Schaefferkoetter JD, Tham IWK, et al: Supervised learning with cycleGAN for low-dose FDG PET image denoising. *Med Image Anal* 65:101770, 2020
 37. Mohammadi I, Castro F, Rahmim A, et al: Motion in nuclear cardiology imaging: types, artifacts, detection and correction techniques. *Phys Med Biol* 67, 2022
 38. Grootjans W, Tixier F, van der Vos CS, et al: The impact of optimal respiratory gating and image noise on evaluation of intratumor heterogeneity on 18F-FDG PET imaging of lung cancer. *J Nucl Med* 57:1692-1698, 2016
 39. Carles M, Bach T, Torres-Espallardo I, et al: Significance of the impact of motion compensation on the variability of PET image features. *Phys Med Biol* 63:065013, 2018
 40. Shiri I, Sanaat A, Salimi Y, et al: PET-QA-NET: Towards routine PET image artifact detection and correction using deep convolutional neural networks. presented at. In: IEEE Nuclear Science Symposium and Medical Imaging Conference (NSS/MIC); 2022/2022
 41. Abdollahi H, Shiri I, Heydari M: Medical imaging technologists in radiomics era: An Alice in Wonderland problem. *Iran J Public Health* 48:184-186, 2019
 42. Oliver JA, Budzevich M, Hunt D, et al: Sensitivity of image features to noise in conventional and respiratory-gated PET/CT images of lung cancer: Uncorrelated noise effects. *Technol Cancer Res Treat* 16:595-608, 2017
 43. Shiri I, Rahmim A, Ghaffarian P, et al: The impact of image reconstruction settings on 18F-FDG PET radiomic features: Multi-scanner phantom and patient studies. *Eur Radiol* 27:4498-4509, 2017
 44. Edalat-Javid M, Shiri I, Hajianfar G, et al: Cardiac SPECT radiomic features repeatability and reproducibility: A multi-scanner phantom study. *J Nucl Cardiol* 28:2730-2744, 2021
 45. van Velden FH, Kramer GM, Frings V, et al: Repeatability of radiomic features in non-small-cell lung cancer [(18)F]FDG-PET/CT studies: Impact of reconstruction and delineation. *Mol Imaging Biol* 18:788-795, 2016
 46. Desserot MC, Tixier F, Weber WA, et al: Reliability of PET/CT shape and heterogeneity features in functional and morphologic components of non-small cell lung cancer tumors: A repeatability analysis in a prospective multicenter cohort. *J Nucl Med* 58:406-411, 2017
 47. Ger RB, Meier JG, Pahlka RB, et al: Effects of alterations in positron emission tomography imaging parameters on radiomics features. *PLoS One* 14:e0221877, 2019
 48. Shiri I, Arabi H, Sanaat A, et al: Fully automated gross tumor volume delineation from PET in head and neck cancer using deep learning algorithms. *Clin Nucl Med* 46:872-883, 2021
 49. Schwyzer M, Ferraro DA, Muehlematter UJ, et al: Automated detection of lung cancer at ultralow dose PET/CT by deep neural networks - Initial results. *Lung Cancer* 126:170-173, 2018
 50. Zhong Z, Kim Y, Plichta K, et al: Simultaneous cosegmentation of tumors in PET-CT images using deep fully convolutional networks. *Med Phys* 46:619-633, 2019

51. Leung KH, Marshdeh W, Wray R, et al: A physics-guided modular deep-learning based automated framework for tumor segmentation in PET. *Phys Med Biol* 65:245032, 2020
52. Bi L, Fulham M, Li N, et al: Recurrent feature fusion learning for multi-modality pet-ct tumor segmentation. *Comput Methods Programs Biomed* 203:106043, 2021
53. Fu X, Bi L, Kumar A, et al: Multimodal Spatial Attention Module for Targeting Multimodal PET-CT Lung Tumor Segmentation. *IEEE J Biomed Health Inform* 25:3507-3516, 2021
54. Yang F, Simpson G, Young L, et al: Impact of contouring variability on oncological PET radiomics features in the lung. *Sci Rep* 10:369, 2020
55. Pfähler E, Mesotten L, Kramer G, et al: Repeatability of two semi-automatic artificial intelligence approaches for tumor segmentation in PET. *EJNMMI Res* 11:4, 2021
56. Zwanenburg A, Leger S, Vallières M, et al: Image biomarker standardisation initiative. *arXiv preprint arXiv 2016:161207003*
57. Leijenaar RT, Nalbantov G, Carvalho S, et al: The effect of SUV discretization in quantitative FDG-PET Radiomics: the need for standardized methodology in tumor texture analysis. *Sci Rep* 5:11075, 2015
58. Yang F, Young LA, Johnson PB: Quantitative radiomics: Validating image textural features for oncological PET in lung cancer. *Radiother Oncol* 129:209-217, 2018
59. Forgács A, Béresová M, Garai I, et al: Impact of intensity discretization on textural indices of [(18)F]FDG-PET tumour heterogeneity in lung cancer patients. *Phys Med Biol* 64:125016, 2019
60. Hosseini SA, Shiri I, Hajianfar G, et al: The impact of preprocessing on the PET-CT radiomics features in non-small cell lung cancer. *Front Biomed Technol* 8:261-272, 2021
61. Klyuzhin IS, Xu Y, Ortiz A, et al: Testing the ability of convolutional neural networks to learn radiomic features. *medRxiv* 2020.09.19.20198077 (preprint)
62. Avard E, Shiri I, Hajianfar G, et al: Non-contrast Cine Cardiac Magnetic Resonance image radiomics features and machine learning algorithms for myocardial infarction detection. *Comput Biol Med* 141:105145, 2022
63. Khodabakhshi Z, Mostafaei S, Arabi H, et al: Non-small cell lung carcinoma histopathological subtype phenotyping using high-dimensional multinomial multiclass CT radiomics signature. *Comput Biol Med* 136:104752, 2021
64. S PS, I S, A HK, et al: Predicting lung cancer patients' survival time via logistic regression-based models in a quantitative radiomic framework. *J Biomed Phys Eng* 10:479-492, 2020
65. Shiri I, Maleki H, Hajianfar G, et al: Next-generation radiogenomics sequencing for prediction of EGFR and KRAS mutation status in NSCLC patients using multimodal imaging and machine learning algorithms. *Mol Imaging Biol* 22:1132-1148, 2020
66. Shiri I, Maleki H, Hajianfar G, et al: PET/CT radiomic sequencer for prediction of EGFR and KRAS mutation status in NSCLC patients presented at IEEE 2018:1-4, 2018
67. Bradshaw TJ, Boellaard R, Dutta J, et al: Nuclear medicine and artificial intelligence: Best practices for algorithm development. *J Nucl Med: jnumed* 121:262567, 2021
68. Shiri I, Salimi Y, Pakbin M, et al: COVID-19 prognostic modeling using CT radiomic features and machine learning algorithms: Analysis of a multi-institutional dataset of 14,339 Patients (preprint). *medRxiv* 2021.12.07.21267364
69. Khodabakhshi Z, Amini M, Mostafaei S, et al: Overall survival prediction in renal cell carcinoma patients using computed tomography radiomic and clinical information. *J Digit Imaging* 34:1086-1098, 2021
70. Shiri I, Salimi Y, Saberi A, et al: Diagnosis of COVID-19 using CT image radiomics features: A comprehensive machine learning study involving 26,307 patients (preprint). *medRxiv* 2021. 2021.12.07.21267367
71. Shiri I, Amini M, Nazari M, et al: Impact of feature harmonization on radiogenomics analysis: Prediction of EGFR and KRAS mutations from non-small cell lung cancer PET/CT images. *Comput Biol Med* 142:105230, 2022
72. Shayesteh S, Nazari M, Salahshour A, et al: Treatment response prediction using MRI-based pre-, post-, and delta-radiomic features and machine learning algorithms in colorectal cancer. *Med Phys* 48:3691-3701, 2021
73. Beauregard JM, Rahmim A: Harmonization of nomenclature for molecular imaging metrics of tumour burden: molecular tumour volume (MTV), total lesion activity (TLA) and total lesion fraction (TLF). *Eur J Nucl Med Mol Imaging* 49:424-426, 2022
74. Bergen RV, Rajotte J-F, Yousefirizi F, et al: 3-D PET Image Generation with tumour masks using TGAN (preprint). *arXiv preprint arXiv 211101866*, 2021. 02TR02 (preprint)
75. Hasani N, Farhadi F, Morris MA, et al: Artificial Intelligence in Medical Imaging and its Impact on the Rare Disease Community: Threats, Challenges and Opportunities. *PET Clin* 17:13-29, 2022. Ahead of print 10.1097/RLU.0000000000004194
76. Hasani N, Morris MA, Rhamim A, et al: Trustworthy Artificial Intelligence in Medical Imaging. *PET Clin* 17:1-12, 2022
77. Shiri I, Vafaei Sadr A, Amini M, et al: Decentralized distributed multi-institutional PET image segmentation using a federated deep learning framework. *Clin Nucl Med* 47:606-617, 2022
78. Shiri I, Vafaei Sadr A, Sanaat A, et al: Federated learning-based deep learning model for PET attenuation and scatter correction: A multi-center study presented at. In: *IEEE Nuclear Science Symposium and Medical Imaging Conference (NSS/MIC); 2022*2022
79. Amini M, Nazari M, Shiri I, et al: Multi-level multi-modality (PET and CT) fusion radiomics: prognostic modeling for non-small cell lung carcinoma. *Phys Med Biol* 66:205017, 2021
80. Amini M, Nazari M, Shiri I, et al: Multi-Level PET and CT Fusion Radiomics-based Survival Analysis of NSCLC Patients presented at IEEE: 1-4, 2020
81. Amini M, Hajianfar G, Hadadi Avval A, et al: Overall survival prognostic modelling of non-small cell lung cancer patients using positron emission tomography/computed tomography harmonised radiomics features: The quest for the optimal machine learning algorithm. *Clin Oncol (R Coll Radiol)* 34:114-127, 2022
82. Khodabakhshi Z, Amini M, Hajianfar G, et al: Histopathological subtype phenotype decoding using harmonized PET/CT image radiomics features and machine learning. presented at IEEE, , Session: M-05 - MIC-Poster I, 21 Oct 2021
83. Lopci E, Kobe C, Gnanasegaran G, et al: PET/CT variants and pitfalls in lung cancer and mesothelioma. *Semin Nucl Med* 51:458-473, 2021
84. Chen L, Liu K, Zhao X, et al: Habitat imaging-based (18)F-FDG PET/CT radiomics for the preoperative discrimination of non-small cell lung cancer and benign inflammatory diseases. *Front Oncol* 11:759897, 2021
85. Ruiz-Cordero R, Devine WP: Targeted Therapy and Checkpoint Immunotherapy in Lung Cancer. *Surg Pathol Clin* 13:17-33, 2020
86. Wyker A, Henderson WW. Solitary Pulmonary Nodule. *Treasure Island (FL): StatPearls Publishing*. Updated 2021 Dec 28. Accessed 2022 Feb 02, Available at: <https://www.ncbi.nlm.nih.gov/books/NBK556143>
87. Truong MT, Ko JP, Rossi SE, et al: Update in the evaluation of the solitary pulmonary nodule. *Radiographics* 34:1658-1679, 2014
88. Mazzone PJ, Gould MK, Arenberg DA, et al: Management of lung nodules and lung cancer screening during the COVID-19 pandemic: CHEST expert panel report. *Chest* 158:406-415, 2020
89. Jonas DE, Reuland DS, Reddy SM, et al: Screening for lung cancer with low-dose computed tomography: Updated evidence report and systematic review for the US preventive services task force. *Jama* 325:971-987, 2021
90. Li P, Wang S, Li T, et al: The cancer imaging archive (TCIA): Maintaining and operating a public information repository. *J Digit Imaging* 26:1045-1057, 2021
91. Clark K, Vendt B, Smith K, et al: The Cancer Imaging Archive (TCIA): Maintaining and Operating a Public Information Repository. *J Digit Imaging* 26:1045-1057, 2013
92. Gu D, Liu G, Xue Z: On the performance of lung nodule detection, segmentation and classification. *Comput Med Imaging Graph* 89:101886, 2021
93. Guo HY, Lin JT, Huang HH, et al: Development and validation of a (18)F-FDG PET/CT-based clinical prediction model for estimating

- malignancy in solid pulmonary nodules based on a population with high prevalence of malignancy. *Clin Lung Cancer* 21:47-55, 2020
94. Zhang R, Zhu L, Cai Z, et al: Potential feature exploration and model development based on 18F-FDG PET/CT images for differentiating benign and malignant lung lesions. *Eur J Radiol* 121:108735, 2019
 95. Park YJ, Choi D, Choi JY, et al: Performance evaluation of a deep learning system for differential diagnosis of lung cancer with conventional CT and FDG PET/CT using transfer learning and metadata. *Clin Nucl Med* 46:635-640, 2021
 96. Niu R, Gao J, Shao X, et al: Maximum standardized uptake value of (18)F-deoxyglucose PET imaging increases the effectiveness of CT radiomics in differentiating benign and malignant pulmonary ground-glass nodules. *Front Oncol* 11:727094, 2021
 97. Gilbert FJ, Harris S, Miles KA, et al: Comparative accuracy and cost-effectiveness of dynamic contrast-enhanced CT and positron emission tomography in the characterisation of solitary pulmonary nodules. *Thorax* 2021:216948. [thoraxjnl-2021-216948](https://doi.org/10.1136/thoraxjnl-2021-216948)
 98. Nichols KJ, DiFilippo FP, Palestro CJ: Computational approaches to detect small lesions in (18) F-FDG PET/CT scans. *J Appl Clin Med Phys* 22:125-139, 2021
 99. Mehranian A, Wollenweber SD, Walker MD, et al: Image enhancement of whole-body oncology [(18)F]-FDG PET scans using deep neural networks to reduce noise. *Eur J Nucl Med Mol Imaging* 49:539-549, 2022
 100. Schwyzer M, Martini K, Benz DC, et al: Artificial intelligence for detecting small FDG-positive lung nodules in digital PET/CT: impact of image reconstructions on diagnostic performance. *Eur Radiol* 30:2031-2040, 2020
 101. Kandathil A, Kay FU, Butt YM, et al: Role of FDG PET/CT in the eighth edition of TNM staging of non-small cell lung cancer. *Radiographics* 38:2134-2149, 2018
 102. Hu Y, Zhao X, Zhang J, et al: Value of 18F-FDG PET/CT radiomic features to distinguish solitary lung adenocarcinoma from tuberculosis. *Eur J Nucl Med Mol Imaging* 48:231-240, 2021
 103. Du D, Gu J, Chen X, et al: Integration of PET/CT radiomics and semantic features for differentiation between active pulmonary tuberculosis and lung cancer. *Mol Imaging Biol* 23:287-298, 2021
 104. Kang F, Mu W, Gong J, et al: Integrating manual diagnosis into radiomics for reducing the false positive rate of 18F-FDG PET/CT diagnosis in patients with suspected lung cancer. *Eur J Nucl Med Mol Imaging* 46:2770-2779, 2019
 105. Watanabe S, Hirata K, Manabe O, et al: A radiomics approach to discriminate lung cancer from pneumonia on FDG PET-CT. *J Nucl Med* 59:1353, 2018. -1353
 106. Guo N, Guo Z, Shusharina N, et al: SVM based radiomics analysis using pre-radiotherapy PET/CT increases the prediction accuracy of radiation pneumonitis. *J Nucl Med* 58:501, 2017. -501
 107. Chen S, Harmon S, Perk T, et al: Diagnostic classification of solitary pulmonary nodules using dual time (18)F-FDG PET/CT image texture features in granuloma-endemic regions. *Sci Rep* 7:9370, 2017. -9370
 108. Chen S, Harmon S, Perk T, et al: Using neighborhood gray tone difference matrix texture features on dual time point PET/CT images to differentiate malignant from benign FDG-avid solitary pulmonary nodules. *Cancer Imaging* 19:56, 2019
 109. Nakajo M, Jinguji M, Aoki M, et al: The clinical value of texture analysis of dual-time-point 18F-FDG-PET/CT imaging to differentiate between 18F-FDG-avid benign and malignant pulmonary lesions. *Eur Radiol* 30:1759-1769, 2020
 110. Teramoto A, Fujita H, Yamamuro O, et al: Automated detection of pulmonary nodules in PET/CT images: Ensemble false-positive reduction using a convolutional neural network technique. *Med Phys* 43:2821-2827, 2016
 111. Zhang X, Sariipan MI, Xu S, et al. Deep Learning PET/CT-Based Radiomics Integrates Clinical Data: Application to Distinguish between Active Pneumonia and Lung Cancer. Updated 2021 Dec 19. Accessed 2022 Feb 02, Available at: <https://ssrn.com/abstract=4001782>
 112. Senent-Valero M, Librero J, Pastor-Valero M: Solitary pulmonary nodule malignancy predictive models applicable to routine clinical practice: a systematic review. *Syst Rev* 10:308, 2021
 113. Krarup MMK, Krokos G, Subesinghe M, et al: Artificial intelligence for the characterization of pulmonary nodules, lung tumors and mediastinal nodes on PET/CT. *Semin Nucl Med* 51:143-156, 2021
 114. Shao X, Niu R, Shao X, et al: Application of dual-stream 3D convolutional neural network based on (18)F-FDG PET/CT in distinguishing benign and invasive adenocarcinoma in ground-glass lung nodules. *EJNMMI Phys* 8:74, 2021
 115. Wu J, Tan Y, Chen Z, et al: Decision based on big data research for non-small cell lung cancer in medical artificial system in developing country. *Comput Methods Programs Biomed* 159:87-101, 2018
 116. Kirienco M, Biroli M, Gelardi F, et al: Deep learning in Nuclear Medicine—focus on CNN-based approaches for PET/CT and PET/MR: where do we stand? *Clin Transl Imaging* 9:37-55, 2021
 117. Han Y, Ma Y, Wu Z, et al: Histologic subtype classification of non-small cell lung cancer using PET/CT images. *Eur J Nucl Med Mol Imaging* 48:350-360, 2021
 118. Koyasu S, Nishio M, Isoda H, et al: Usefulness of gradient tree boosting for predicting histological subtype and EGFR mutation status of non-small cell lung cancer on 18F FDG-PET/CT. *Ann Nucl Med* 34:49-57, 2020
 119. Ma Y, Feng W, Wu Z, et al: Intra-tumoural heterogeneity characterization through texture and colour analysis for differentiation of non-small cell lung carcinoma subtypes. *Phys Med Biol* 63:165018, 2018
 120. Kirienco M, Cozzi L, Rossi A, et al: Ability of FDG PET and CT radiomics features to differentiate between primary and metastatic lung lesions. *Eur J Nucl Med Mol Imaging* 45:1649-1660, 2018
 121. Ren C, Zhang J, Qi M, et al: Machine learning based on clinico-biological features integrated 18F-FDG PET/CT radiomics for distinguishing squamous cell carcinoma from adenocarcinoma of lung. *Eur J Nucl Med Mol Imaging* 48:1538-1549, 2021
 122. Ji Y, Qiu Q, Fu J, et al: Stage-specific PET radiomic prediction model for the histological subtype classification of non-small-cell lung cancer. *Cancer Manage Res* 13:307-317, 2021
 123. Sha X, Gong G, Qiu Q, et al: Identifying pathological subtypes of non-small-cell lung cancer by using the radiomic features of 18F-fluoro-deoxyglucose positron emission computed tomography. *Transl Cancer Res* 8:1741-1749, 2019
 124. Yan M, Wang W: Development of a radiomics prediction model for histological type diagnosis in solitary pulmonary nodules: The combination of CT and FDG PET. *Front Oncol* 10:555514, 2020
 125. Zhou Y, Ma XL, Zhang T, et al: Use of radiomics based on 18F-FDG PET/CT and machine learning methods to aid clinical decision-making in the classification of solitary pulmonary lesions: an innovative approach. *Eur J Nucl Med Mol Imaging* 48:2904-2913, 2021
 126. Li J, mu w, Tian J, et al: The malignant/benign differential diagnosis value of different 18F-FDG PET/CT radiomics nomograms in solitary pulmonary lesions. *J Nucl Med* 59:1348, 2018. -1348
 127. Verschakelen JA, Bogaert J, De Wever W: Computed tomography in staging for lung cancer. *Eur Respir J Suppl* 35:40s-48s, 2002
 128. Quint LE: Staging non-small cell lung cancer. *Cancer Imaging* 7:148-159, 2007
 129. Cuaron J, Dunphy M, Rimner A: Role of FDG-PET scans in staging, response assessment, and follow-up care for non-small cell lung cancer. *Front Oncol* 2:208, 2012
 130. Kirienco M, Gallivanone F, Sollini M, et al: FDG PET/CT as theranostic imaging in diagnosis of non-small cell lung cancer. *Front Biosci (Landmark Ed)* 22:1713-1723, 2017
 131. Kirienco M, Sollini M, Silvestri G, et al: Convolutional neural networks promising in lung cancer T-parameter assessment on baseline FDG-PET/CT. *Contrast Media Mol Imaging* 2018:1382309, 2018
 132. Ashok A, Jiwnani SS, Karimundackal G, et al: Controversies in mediastinal staging for non-small cell lung cancer. *Indian J Med Paediatr Oncol* 42:406-414, 2021
 133. Seol HY, Kim YS, Kim SJ: Predictive value of 18F-fluorodeoxyglucose positron emission tomography or positron emission tomography/computed tomography for assessment of occult lymph node metastasis in non-small cell lung cancer. *Oncology* 99:96-104, 2021

134. Pak K, Park S, Cheon GJ, et al: Update on nodal staging in non-small cell lung cancer with integrated positron emission tomography/computed tomography: A meta-analysis. *Ann Nucl Med* 29:409-419, 2015
135. Shen G, Lan Y, Zhang K, et al: Comparison of 18F-FDG PET/CT and DWI for detection of mediastinal nodal metastasis in non-small cell lung cancer: A meta-analysis. *PLoS One* 12:e0173104, 2017
136. Vincent BD, El-Bayoumi E, Hoffman B, et al: Real-time endobronchial ultrasound-guided transbronchial lymph node aspiration. *Ann Thorac Surg* 85:224-230, 2008
137. Remon J, Soria JC, Peters S: Early and locally advanced non-small-cell lung cancer: An update of the ESMO Clinical Practice Guidelines focusing on diagnosis, staging, systemic and local therapy. *Ann Oncol* 32:1637-1642, 2021
138. Flechsig P, Frank P, Kratochwil C, et al: Radiomic analysis using density threshold for FDG-PET/CT-based N-staging in lung cancer patients. *Mol Imaging Biol* 19:315-322, 2017
139. Vesselle H, Turcotte E, Wiens L, et al: Application of a neural network to improve nodal staging accuracy with 18F-FDG PET in non-small cell lung cancer. *J Nucl Med* 44:1918-1926, 2003
140. Pak K, Kim K, Kim MH, et al: A decision tree model for predicting mediastinal lymph node metastasis in non-small cell lung cancer with F-18 FDG PET/CT. *PLoS ONE* 13:e0193403, 2018
141. Wu Y, Liu J, Han C, et al: Preoperative prediction of lymph node metastasis in patients with early-T-stage non-small cell lung cancer by machine learning algorithms. *Front Oncol* 10:743, 2020
142. Kawaguchi Y, Matsuura Y, Kondo Y, et al: The predictive power of artificial intelligence on mediastinal lymphnode metastasis. *Gen Thorac Cardiovasc Surg* 69:1545-1552, 2021
143. Nie P, Yang G, Wang N, et al: Additional value of metabolic parameters to PET/CT-based radiomics nomogram in predicting lymphovascular invasion and outcome in lung adenocarcinoma. *Eur J Nucl Med Mol Imaging* 48:217-230, 2021
144. Gao X, Chu C, Li Y, et al: The method and efficacy of support vector machine classifiers based on texture features and multi-resolution histogram from (18)F-FDG PET-CT images for the evaluation of mediastinal lymph nodes in patients with lung cancer. *Eur J Radiol* 84:312-317, 2015
145. Zheng K, Wang X, Jiang C, et al: Pre-operative prediction of mediastinal node metastasis using radiomics model based on (18)F-FDG PET/CT of the primary tumor in non-small cell lung cancer patients. *Front Med (Lausanne)* 8:673876, 2021
146. Wang H, Zhou Z, Li Y, et al: Comparison of machine learning methods for classifying mediastinal lymph node metastasis of non-small cell lung cancer from 18F-FDG PET/CT images. *EJNMMI Res* 7:11, 2017
147. Yoo J, Cheon M, Park YJ, et al: Machine learning-based diagnostic method of pre-therapeutic 18F-FDG PET/CT for evaluating mediastinal lymph nodes in non-small cell lung cancer. *Eur Radiol* 31:4184-4194, 2021
148. Taralli S, Scolozzi V, Boldrini L, et al: Application of artificial neural network to preoperative (18)F-FDG PET/CT for predicting pathological nodal involvement in non-small-cell lung cancer patients. *Front Med (Lausanne)* 8:664529, 2021
149. Chang C, Ruan M, Chen C, et al: Development of a PET/CT molecular radiomics-clinical model to predict local lymph node metastasis of invasive lung adenocarcinoma (≤ 3 cm)(preprint). *Research Square*: 1-19, 2021
150. Ouyang ML, Tang K, Xu MM, et al: Prediction of occult lymph node metastasis using tumor-to-blood standardized uptake ratio and metabolic parameters in clinical N0 lung adenocarcinoma. *Clin Nucl Med* 43:715-720, 2018
151. Kim DH, Song BI, Hong CM, et al: Metabolic parameters using ¹⁸F-FDG PET/CT correlate with occult lymph node metastasis in squamous cell lung carcinoma. *Eur J Nucl Med Mol Imaging* 41:2051-2057, 2014
152. Tau N, Stundzia A, Yasufuku K, et al: Convolutional neural networks in predicting nodal and distant metastatic potential of newly diagnosed non-small cell lung cancer on FDG PET images. *Am J Roentgenol* 215:192-197, 2020
153. Lyu L, Wu N: PET/CT-based radiomics signature for predicting occult lymph node metastasis in clinical stage I lung adenocarcinoma. *J Nucl Med* 61:1345, 2020. -1345
154. Wallis D, Soussan M, Lacroix M, et al: An [18F]FDG-PET/CT deep learning method for fully automated detection of pathological mediastinal lymph nodes in lung cancer patients. *Eur J Nucl Med Mol Imaging* 49:881-888, 2021
155. Churchill IF, Sullivan KA, Simone AC, et al: Thoracic imaging radiomics for staging lung cancer: a systematic review and radiomic quality assessment. *Clin Transl Imaging* 10:191-216, 2021
156. Qu X, Huang X, Yan W, et al: A meta-analysis of ¹⁸F-FDG-PET-CT, ¹⁸F-FDG-PET, MRI and bone scintigraphy for diagnosis of bone metastases in patients with lung cancer. *Eur J Radiol* 81:1007-1015, 2012
157. Wu Y, Li P, Zhang H, et al: Diagnostic value of fluorine 18 fluorodeoxyglucose positron emission tomography/computed tomography for the detection of metastases in non-small-cell lung cancer patients. *Int J Cancer* 132:E37-E47, 2013
158. Coroller T, Yip S, Kim J, et al: SU-D-207B-03: A PET-CT radiomics comparison to predict distant metastasis in lung adenocarcinoma. *J Med Phys* 43:3349, 2016. -3349
159. Wu J, Aguilera T, Shultz D, et al: Early-stage non-small cell lung cancer: Quantitative imaging characteristics of (18)F fluorodeoxyglucose PET/CT allow prediction of distant metastasis. *Radiology* 281:270-278, 2016
160. Parikh AR: Lung Cancer Genomics. *Acta Med Acad* 48:78-83, 2019
161. Imyanitov EN, Iyevleva AG, Levchenko EV: Molecular testing and targeted therapy for non-small cell lung cancer: Current status and perspectives. *Crit Rev Oncol Hematol* 157:103194, 2021
162. Novikov M: Multiparametric quantitative and texture 18F-FDG PET/CT analysis for primary malignant tumour grade differentiation. *Eur Radiol Exp* 3:48, 2019
163. Sanduleanu S, Jochems A, Upadhaya T, et al: Non-invasive imaging prediction of tumor hypoxia: A novel developed and externally validated CT and FDG-PET-based radiomic signatures. *Radiother Oncol* 153:97-105, 2020
164. Moon SH, Kim J, Joung JG, et al: Correlations between metabolic texture features, genetic heterogeneity, and mutation burden in patients with lung cancer. *Eur J Nucl Med Mol Imaging* 46:446-454, 2019
165. Kim G, Kim J, Cha H, et al: Metabolic radiogenomics in lung cancer: associations between FDG PET image features and oncogenic signaling pathway alterations. *Sci Rep* 10:13231, 2020
166. Chapman AM, Sun KY, Ruestow P, et al: Lung cancer mutation profile of EGFR, ALK, and KRAS: Meta-analysis and comparison of never and ever smokers. *Lung Cancer* 102:122-134, 2016
167. Zhang L, Chen B, Liu X, et al: Quantitative biomarkers for prediction of epidermal growth factor receptor mutation in non-small cell lung cancer. *Transl Oncol* 11:94-101, 2018
168. Li X, Yin G, Zhang Y, et al: Predictive power of a radiomic signature based on 18F-FDG PET/CT images for EGFR mutational status in NSCLC. *Front Oncol* 9:1062, 2019
169. Zhang J, Zhao X, Zhao Y, et al: Value of pre-therapy 18F-FDG PET/CT radiomics in predicting EGFR mutation status in patients with non-small cell lung cancer. *Eur J Nucl Med Mol Imaging* 47:1137-1146, 2020
170. Nair JKR, Saeed UA, McDougall CC, et al: Radiogenomic models using machine learning techniques to predict EGFR mutations in non-small cell lung cancer. *Can Assoc Radiol J* 72:109-119, 2021
171. Shirri I, Maleki H, Hajianfar G, et al: Next-generation radiogenomics sequencing for prediction of EGFR and KRAS mutation status in NSCLC patients using multimodal imaging and machine learning algorithms. *Mol Imaging Biol* 22:1132-1148, 2020
172. Yip SSF, Kim J, Coroller TP, et al: Associations between somatic mutations and metabolic imaging phenotypes in non-small cell lung cancer. *J Nucl Med* 58:569-576, 2017
173. Yip SSF, Parmar C, Kim J, et al: Impact of experimental design on PET radiomics in predicting somatic mutation status. *Eur J Radiol* 97:8-15, 2017
174. Whi W, Ha S, Bae S, et al: Relationship of EGFR mutation to glucose metabolic activity and asphericity of metabolic tumor volume in lung adenocarcinoma. *Nucl Med Mol Imaging* 54:175-182, 2020

175. Yin G, Wang Z, Song Y, et al: Prediction of EGFR mutation status based on 18F-FDG PET/CT imaging using deep learning-based model in lung adenocarcinoma. *Front Oncol* 11:709137, 2021
176. Chang C, Zhou S, Yu H, et al: A clinically practical radiomics-clinical combined model based on PET/CT data and nomogram predicts EGFR mutation in lung adenocarcinoma. *Eur Radiol* 31:6259-6268, 2021
177. Mu W, Jiang L, Zhang JY, et al: Non-invasive decision support for NSCLC treatment using PET/CT radiomics. *Nat Commun* 11:5228, 2020
178. Jiang M, Zhang Y, Xu J, et al: Assessing EGFR gene mutation status in non-small cell lung cancer with imaging features from PET/CT. *Nucl Med Commun* 40:842-849, 2019
179. Wang H, Huang J, Yu X, et al: Different efficacy of EGFR tyrosine kinase inhibitors and prognosis in patients with subtypes of EGFR-mutated advanced non-small cell lung cancer: a meta-analysis. *J Cancer Res Clin Oncol* 140:1901-1909, 2014
180. Yang B, Ji HS, Zhou CS, et al: (18)F-fluorodeoxyglucose positron emission tomography/computed tomography-based radiomic features for prediction of epidermal growth factor receptor mutation status and prognosis in patients with lung adenocarcinoma. *Transl Lung Cancer Res* 9:563-574, 2020
181. Liu Q, Sun D, Li N, et al: Predicting EGFR mutation subtypes in lung adenocarcinoma using 18F-FDG PET/CT radiomic features. *Transl Lung Cancer Res* 9:549-562, 2020
182. Zhang M, Bao Y, Rui W, et al: Performance of 18F-FDG PET/CT radiomics for predicting EGFR mutation status in patients with non-small cell lung cancer. *Front Oncol* 10:568857, 2020
183. Chen Q, Zhang L, Mo X, et al: Current status and quality of radiomic studies for predicting immunotherapy response and outcome in patients with non-small cell lung cancer: a systematic review and meta-analysis. *Eur J Nucl Med Mol Imaging* 49:345-360, 2021
184. Li J, Ge S, Sang S, et al: Evaluation of PD-L1 expression level in patients with non-small cell lung cancer by (18)F-FDG PET/CT radiomics and clinicopathological characteristics. *Front Oncol* 11:789014, 2021
185. Zhou J, Zou S, Kuang D, et al: A novel approach using FDG-PET/CT-based radiomics to assess tumor immune phenotypes in patients with non-small cell lung cancer. *Front Oncol* 11:769272, 2021
186. Jiang M, Sun D, Guo Y, et al: Assessing PD-L1 expression level by radiomic features from PET/CT in non small cell lung cancer patients: An initial result. *Acad Radiol* 27:171-179, 2020
187. Chang C, Sun X, Wang G, et al: A machine learning model based on PET/CT radiomics and clinical characteristics predicts ALK rearrangement status in lung adenocarcinoma. *Front Oncol* 11:603882, 2021
188. Yoon HJ, Sohn I, Cho JH, et al: Decoding Tumor Phenotypes for ALK, ROS1, and RET fusions in lung adenocarcinoma using a radiomics approach. *Medicine (Baltimore)* 94:e1753, 2015
189. Moitra D, Mandal RK: Automated grading of non-small cell lung cancer by fuzzy rough nearest neighbour method. *Netw Model Anal Health Informatics Bioinformatics* 8:1-9, 2019
190. Palumbo B, Capozzi R, Bianconi F, et al: Classification model to estimate MIB-1 (Ki 67) proliferation index in NSCLC patients evaluated with 18F-FDG-PET/CT. *Anticancer Res* 40:3355-3360, 2020
191. La Greca Saint-Estevan A, Vuong D, Tschanz F, et al: Systematic review on the association of radiomics with tumor biological endpoints. *Cancers (Basel)* 13:3015, 2021
192. van Zandwijk N, Mooi WJ, Rodenhuis S: Prognostic factors in NSCLC. Recent experiences. *Lung Cancer* 12(Suppl 1):S27-S33, 1995
193. Pennell NA, Arcila ME, Gandara DR, et al: Biomarker testing for patients with advanced non-small cell lung cancer: Real-world issues and tough choices. *Am Soc Clin Oncol Educ Book* 39:531-542, 2019
194. Dziedzic DA, Rudzinski P, Langfort R, et al: Risk factors for local and distant recurrence after surgical treatment in patients with non-small-cell lung cancer. *Clin Lung Cancer* 17:e157-e167, 2016
195. Deng HY, Zheng X, Jiang R, et al: Preoperative D-dimer level is an independent prognostic factor for non-small cell lung cancer after surgical resection: a systematic review and meta-analysis. *Ann Transl Med* 7:366, 2019
196. Lee HY, Lee SW, Lee KS, et al: Role of CT and PET Imaging in Predicting Tumor Recurrence and Survival in Patients with Lung Adenocarcinoma: A Comparison with the International Association for the Study of Lung Cancer/American Thoracic Society/European Respiratory Society Classification of Lung Adenocarcinoma. *J Thorac Oncol* 10:1785-1794, 2015
197. Ko KH, Hsu HH, Huang TW, et al: Predictive value of 18F-FDG PET and CT morphologic features for recurrence in pathological stage IA non-small cell lung cancer. *Medicine (Baltimore)* 94:e434, 2015
198. de Geus-Oei LF, van der Heijden HF, Corstens FH, et al: Predictive and prognostic value of FDG-PET in non small-cell lung cancer: A systematic review. *Cancer* 110:1654-1664, 2007
199. Liu J, Dong M, Sun X, et al: Prognostic value of 18F-FDG PET/CT in surgical non-small cell lung cancer: A meta-analysis. *PLoS ONE* 11: e0146195, 2016
200. Mattonen SA, Davidzon GA, Bakr S, et al: [18F] fdg positron emission tomography (Pet) tumor and penumbra imaging features predict recurrence in non-small cell lung cancer. *Tomography* 5:145-153, 2019
201. Tixier F, Hatt M, Valla C, et al: Visual versus quantitative assessment of intratumor 18F-FDG PET uptake heterogeneity: prognostic value in non-small cell lung cancer. *J Nucl Med* 55:1235-1241, 2014
202. Cook GJ, O'Brien ME, Siddique M, et al: Non-small cell lung cancer treated with erlotinib: Heterogeneity of (18)F-FDG uptake at PET-association with treatment response and prognosis. *Radiology* 276:883-893, 2015
203. Lovinfosse P, January ZL, Coucke P, et al: FDG PET/CT texture analysis for predicting the outcome of lung cancer treated by stereotactic body radiation therapy. *Eur J Nucl Med Mol Imaging* 43:1453-1460, 2016
204. Pyka T, Bundschuh RA, Andratschke N, et al: Textural features in pretreatment [F18]-FDG-PET/CT are correlated with risk of local recurrence and disease-specific survival in early stage NSCLC patients receiving primary stereotactic radiation therapy. *Radiat Oncol* 10:100, 2015
205. Takeda K, Takanami K, Shirata Y, et al: Clinical utility of texture analysis of 18F-FDG PET/CT in patients with Stage I lung cancer treated with stereotactic body radiotherapy. *J Rad Res* 58:862-869, 2017
206. Cook GJ, Yip C, Siddique M, et al: Are pretreatment 18F-FDG PET tumor textural features in non-small cell lung cancer associated with response and survival after chemoradiotherapy? *J Nucl Med* 54:19-26, 2013
207. Apostolova I, Rogasch J, Buchert R, et al: Quantitative assessment of the asphericity of pretherapeutic FDG uptake as an independent predictor of outcome in NSCLC. *BMC Cancer* 14:896, 2014
208. Ohri N, Duan F, Snyder BS, et al: Pretreatment 18F-FDG PET textural features in locally advanced non-small cell lung cancer: Secondary analysis of ACRIN 6668/RTOG 0235. *J Nucl Med* 57:842-848, 2016
209. Fried DV, Mawlawi O, Zhang L, et al: Stage III Non-small cell lung cancer: Prognostic value of FDG PET quantitative imaging features combined with clinical prognostic factors. *Radiology* 278:214-222, 2016
210. Jensen GL, Yost CM, Mackin DS, et al: Prognostic value of combining a quantitative image feature from positron emission tomography with clinical factors in oligometastatic non-small cell lung cancer. *Radiother Oncol* 126:362-367, 2018
211. Oikonomou A, Khalvati F, Tyrrell PN, et al: Radiomics analysis at PET/CT contributes to prognosis of recurrence and survival in lung cancer treated with stereotactic body radiotherapy. *Sci Rep* 8:1-11, 2018
212. Dong X, Sun X, Sun L, et al: Early change in metabolic tumor heterogeneity during chemoradiotherapy and its prognostic value for patients with locally advanced non-small cell lung cancer. *PLoS ONE* 11: e0157836, 2016
213. Sepehri S, Tankyevych O, Upadhaya T, et al: Comparison and fusion of machine learning algorithms for prospective validation of PET/CT radiomic features prognostic value in stage II-III non-small cell lung cancer. *Diagn* 11:675, 2021
214. Kirienko M, Cozzi L, Antunovic L, et al: Prediction of disease-free survival by the PET/CT radiomic signature in non-small cell lung cancer

- patients undergoing surgery. *Eur J Nucl Med Mol Imaging* 45:207-217, 2018
215. Krarup MMK, Nygård L, Vogelius IR, et al: Heterogeneity in tumours: Validating the use of radiomic features on 18F-FDG PET/CT scans of lung cancer patients as a prognostic tool. *Radiother Oncol* 144:72-78, 2020
216. Konert T, Everitt S, La Fontaine MD, et al: Robust, independent and relevant prognostic 18F-fluorodeoxyglucose positron emission tomography radiomics features in non-small cell lung cancer: Are there any? *PLoS ONE* 15:e0228793, 2020
217. Ijsseldijk MA, Shoni M, Siegert C, et al: Oncologic outcomes of surgery versus SBRT for non-small-cell lung carcinoma: A systematic review and meta-analysis. *Clin Lung Cancer* 22:e235-e292, 2021
218. Montagne F, Guisier F, Venissac N, et al: The role of surgery in lung cancer treatment: Present indications and future perspectives-state of the art. *Cancers (Basel)* 13:3711, 2021
219. Uramoto H, Tanaka F: Recurrence after surgery in patients with NSCLC. *Transl Lung Cancer Res* 3:242-249, 2014
220. Han S, Woo S, Suh CH, et al: A systematic review of the prognostic value of texture analysis in 18F-FDG PET in lung cancer. *Ann Nucl Med* 32:602-610, 2018
221. Nakajo M, Jinguji M, Shinaji T, et al: A pilot study of texture analysis of primary tumor [18F]FDG uptake to predict recurrence in surgically treated patients with non-small cell lung cancer. *Mol Imaging Biol* 21:771-780, 2019
222. Harmon S, Seder CW, Chen S, et al: Quantitative FDG PET/CT may help risk-stratify early-stage non-small cell lung cancer patients at risk for recurrence following anatomic resection. *J Thorac Dis* 11:1106-1116, 2019
223. Ahn HK, Lee H, Kim SG, et al: Pre-treatment 18F-FDG PET-based radiomics predict survival in resected non-small cell lung cancer. *Clin Radiol* 74:467-473, 2019
224. Christie JR, Abdelrazek M, Lang P, et al: A multi-modality radiomics-based model for predicting recurrence in non-small cell lung cancer. In: *Progress in Biomedical Optics and Imaging - Proceedings of SPIE, SPIE*, :116000L2021
225. Lambin P, Rios-Velazquez E, Leijenaar R, et al: Radiomics: Extracting more information from medical images using advanced feature analysis. *Eur J Cancer* 48:441-446, 2012
226. Aerts HJ: The potential of radiomic-based phenotyping in precision medicine: A review. *JAMA Oncol* 2:1636-1642, 2016
227. Mattonen SA, Davidzon GA, Benson J, et al: Bone marrow and tumor radiomics at 18F-FDG PET/CT: Impact on outcome prediction in non-small cell lung cancer. *Radiology* 293:451-459, 2019
228. Mu W, Katsoulakis E, Whelan CJ, et al: Radiomics predicts risk of cachexia in advanced NSCLC patients treated with immune checkpoint inhibitors. *Br J Cancer* 125:229-239, 2021
229. Sollini M, Gelardi F, Matassa G, et al: Interdisciplinarity: An essential requirement for translation of radiomics research into clinical practice -a systematic review focused on thoracic oncology. *Rev Esp Med Nucl Imagen Mol (Engl Ed)* 39:146-156, 2020
230. Kothari G, Korte J, Lehrer EJ, et al: A systematic review and meta-analysis of the prognostic value of radiomics based models in non-small cell lung cancer treated with curative radiotherapy. *Radiother Oncol* 155:188-203, 2021
231. Li H, Becker N, Raman S, et al: The value of nodal information in predicting lung cancer relapse using 4DPET/4DCT. *Med Phys* 42:4727-4733, 2015
232. Li H, Galperin-Aizenberg M, Pryma D, et al: Unsupervised machine learning of radiomic features for predicting treatment response and overall survival of early stage non-small cell lung cancer patients treated with stereotactic body radiation therapy. *Radiother Oncol* 129:218-226, 2018
233. Dissaux G, Visvikis D, Daano R, et al: Pretreatment 18F-FDG PET/CT radiomics predict local recurrence in patients treated with stereotactic body radiotherapy for early-stage non-small cell lung cancer: A multicentric study. *J Nucl Med* 61:814-820, 2020
234. Luo Y, McShan DL, Matuszak MM, et al: A multiobjective Bayesian networks approach for joint prediction of tumor local control and radiation pneumonitis in non-small-cell lung cancer (NSCLC) for response-adapted radiotherapy. *Med Phys* 45:3980-3995, 2018
235. Zhou Z, Folkert M, Iyengar P, et al: Multi-objective radiomics model for predicting distant failure in lung SBRT. *Phys Med Biol* 62:4460-4478, 2017
236. Li S, Yang N, Li B, et al: A pilot study using kernelled support tensor machine for distant failure prediction in lung SBRT. *Med Image Anal* 50:106-116, 2018
237. Hao H, Zhou Z, Wang J: Distant failure prediction for early stage NSCLC by analyzing PET with sparse representation. *Int Soc Optics and Photonics*. 10134:101343W-1-7, 2017
238. Suga M, Nishii R, Miwa K, et al: Differentiation between non-small cell lung cancer and radiation pneumonitis after carbon-ion radiotherapy by 18F-FDG PET/CT texture analysis. *Sci Rep* 11:11509, 2021
239. Lee K, Le T, Hau E, et al: A systematic review into the radiologic features predicting local recurrence after stereotactic ablative body radiotherapy (SABR) in patients with Non-Small Cell Lung Cancer (NSCLC). *Int J Radiat Oncol Biol Phys* 113:40-59, 2021
240. Brooks ED, Verma V, Senan S, et al: Salvage therapy for locoregional recurrence after stereotactic ablative radiotherapy for early-stage NSCLC. *J Thorac Oncol* 15:176-189, 2020
241. Bury T, Corhay JL, Duysinx B, et al: Value of FDG-PET in detecting residual or recurrent non small cell lung cancer. *Eur Respir J* 14:1376-1380, 1999
242. Ulaner GA, Lyall A: Identifying and distinguishing treatment effects and complications from malignancy at FDG PET/CT. *Radiographics* 33:1817-1834, 2013
243. Coroller TP, Agrawal V, Huynh E, et al: Radiomic-based pathological response prediction from primary tumors and lymph nodes in NSCLC. *J Thorac Oncol* 12:467-476, 2017
244. van Laar M, van Amsterdam WAC, van Lindert ASR, et al: Prognostic factors for overall survival of stage III non-small cell lung cancer patients on computed tomography: A systematic review and meta-analysis. *Radiother Oncol* 151:152-175, 2020
245. Guberina M, Eberhardt W, Stuschke M, et al: Pretreatment metabolic tumour volume in stage IIIA/B non-small-cell lung cancer uncovers differences in effectiveness of definitive radiochemotherapy schedules: analysis of the ESPATUE randomized phase 3 trial. *Eur J Nucl Med Mol Imaging* 46:1439-1447, 2019
246. Guberina M, Poettgen C, Metzzenmacher M, et al: Prognostic value of post-induction chemotherapy volumetric pet/ct parameters for stage IIIA/B non-small cell lung cancer patients receiving definitive chemoradiotherapy. *J Nucl Med* 62:1684-1691, 2021
247. Zhang N, Liang R, Gensheimer MF, et al: Early response evaluation using primary tumor and nodal imaging features to predict progression-free survival of locally advanced non-small cell lung cancer. *Theranostics* 10:11707-11718, 2020
248. van Timmeren JE, Carvalho S, Leijenaar RTH, et al: Challenges and caveats of a multi-center retrospective radiomics study: An example of early treatment response assessment for NSCLC patients using FDG-PET/CT radiomics. *PLoS ONE* 14:e0217536, 2019
249. Arshad MA, Thornton A, Lu H, et al: Discovery of pre-therapy 2-deoxy-2-18 F-fluoro-D-glucose positron emission tomography-based radiomics classifiers of survival outcome in non-small-cell lung cancer patients. *Eur J Nucl Med Mol Imaging* 46:455-466, 2019
250. Moran A, Wang Y, Dyer BA, et al: Prognostic value of computed tomography and/or 18F-fluorodeoxyglucose positron emission tomography radiomics features in locally advanced non-small cell lung cancer. *Clin Lung Cancer* 22:461-468, 2021
251. Astaraki M, Wang C, Buizza G, et al: Early survival prediction in non-small cell lung cancer from PET/CT images using an intra-tumor partitioning method. *Phys Med* 60:58-65, 2019
252. Carles M, Fechter T, Radicioni G, et al: Fdg-pet radiomics for response monitoring in non-small-cell lung cancer treated with radiation therapy. *Cancers* 13:1-15, 2021
253. Mu W, Tunalı I, Gray JE, et al: Radiomics of 18F-FDG PET/CT images predicts clinical benefit of advanced NSCLC patients to checkpoint blockade immunotherapy. *Eur J Nucl Med Mol Imaging* 47:1168-1182, 2020

254. Mu W, Jiang L, Shi Y, et al: Non-invasive measurement of PD-L1 status and prediction of immunotherapy response using deep learning of PET/CT images. *J Immunother Cancer* 9:e002118, 2021
255. Ayati N, Lee ST, Zakavi SR, et al: Response evaluation and survival prediction after PD-1 immunotherapy in patients with non-small cell lung cancer: Comparison of assessment methods. *J Nucl Med* 62:926-933, 2021
256. Polverari G, Ceci F, Bertaglia V, et al: 18F-FDG pet parameters and radiomics features analysis in advanced nslc treated with immunotherapy as predictors of therapy response and survival. *Cancers* 12:1163, 2020
257. Valentinuzzi D, Vrankar M, Boc N, et al: FDG PET immunotherapy radiomics signature (iRADIOMICS) predicts response of non-small-cell lung cancer patients treated with pembrolizumab. *Radiol Oncol* 54:285-294, 2020
258. Nakajima EC, Leal JP, Fu W, et al: CT and PET radiomic features associated with major pathologic response to neoadjuvant immunotherapy in early-stage non-small cell lung cancer (NSCLC)[Abstract]. *J Clin Oncol* 38:9031, 2020.. -9031
259. Park C, Na KJ, Choi H, et al: Tumor immune profiles noninvasively estimated by FDG PET with deep learning correlate with immunotherapy response in lung adenocarcinoma. *Theranostics* 10:10838-10848, 2020
260. Du B, Wang S, Cui Y, et al: Can (18)F-FDG PET/CT predict EGFR status in patients with non-small cell lung cancer? A systematic review and meta-analysis. *BMJ Open* 11:e044313, 2021
261. Abdurixiti M, Nijjati M, Shen R, et al: Current progress and quality of radiomic studies for predicting EGFR mutation in patients with non-small cell lung cancer using PET/CT images: A systematic review. *Br J Radiol* 94:20201272, 2021
262. Park S, Ha S, Lee SH, et al: Intratumoral heterogeneity characterized by pretreatment PET in non-small cell lung cancer patients predicts progression-free survival on EGFR tyrosine kinase inhibitor. *PLoS ONE* 13:e0189766, 2018
263. Shao D, Du D, Liu H, et al: Identification of stage IIIC/IV EGFR-mutated non-small cell lung cancer populations sensitive to targeted therapy based on a PET/CT radiomics risk model. *Front Oncol* 11:721318, 2021
264. Chetan MR, Gleeson FV: Radiomics in predicting treatment response in non-small-cell lung cancer: current status, challenges and future perspectives. *Eur Radiol* 31:1049-1058, 2021
265. Walls GM, Osman SOS, Brown KH, et al: Radiomics for predicting lung cancer outcomes following radiotherapy: A Systematic Review. *Clin Oncol (R Coll Radiol)* 34:e107-e122, 2022
266. Vaz SC, Adam JA, Delgado Bolton RC, et al: Joint EANM/SNMMI/ESTRO practice recommendations for the use of 2-[(18)F]FDG PET/CT external beam radiation treatment planning in lung cancer V1.0. *Eur J Nucl Med Mol Imaging* 49:1386-1406, 2022
267. Wang JH, Wahid KA, van Dijk LV, et al: Radiomic biomarkers of tumor immune biology and immunotherapy response. *Clin Transl Radiat Oncol* 28:97-115, 2021
268. Tankyevych O, Tixier F, Antonorsi N, et al: Can alternative PET reconstruction schemes improve the prognostic value of radiomic features in non-small cell lung cancer? *Methods* 188:73-83, 2021
269. Park JE, Kim D, Kim HS, et al: Quality of science and reporting of radiomics in oncologic studies: room for improvement according to radiomics quality score and TRIPOD statement. *Eur Radiol* 30:523-536, 2020
270. Jayakumar S, Sounderajah V, Normahani P, et al: Quality assessment standards in artificial intelligence diagnostic accuracy systematic reviews: a meta-research study. *NPJ Digit Med* 5:11, 2022
271. Moons KG, Altman DG, Reitsma JB, et al: Transparent Reporting of a multivariable prediction model for Individual Prognosis or Diagnosis (TRIPOD): Explanation and elaboration. *Ann Intern Med* 162:W1-73, 2015
272. Murray JM, Wiegand B, Hadaschik B, Herrmann K, Kleesiek J: Virtual Biopsy: Just an AI Software or a Medical Procedure? *J Nucl Med jnumed.121:263749*, 2022